Review

Well-Defined Conjugated Macromolecules Based on Oligo(Arylene Ethynylene)s in Sensing †

Agata Krywko-Cendrowska [1] , **Dawid Szweda** [2] **and Roza Szweda** [2,*]

[1] Department of Chemistry, University of Basel, Mattenstrasse 24a, BPR 1096, 4058 Basel, Switzerland; a.krywko@unibas.ch
[2] Łukasiewicz Research Network–PORT Polish Center for Technology Development, Stabłowicka 147, 54-066 Wrocław, Poland; dawidszweda@gmail.com
* Correspondence: roza.szweda@port.org.pl
† Special Issue on "Bioprocess Monitoring and Control".

check for updates

Abstract: Macromolecules with well-defined structures in terms of molar mass and monomer sequence became interesting building blocks for modern materials. The precision of the macromolecular structure makes fine-tuning of the properties of resulting materials possible. Conjugated macromolecules exhibit excellent optoelectronic properties that make them exceptional candidates for sensor construction. The importance of chain length and monomer sequence is particularly important in conjugated systems. The oligomer length, monomer sequence, and structural modification often influence the energy bang gap between the highest occupied molecular orbital (HOMO) and the lowest unoccupied molecular orbital (LUMO) of the molecules that reflect in their properties. Moreover, the supramolecular aggregation that is often observed in oligo-conjugated systems is usually strongly affected by even minor structural changes that are used for sensor designs. This review discusses the examples of well-defined conjugated macromolecules based on oligo(arylene ethynylene) skeleton used for sensor applications. Here, exclusively examples of uniform macromolecules are summarized. The sensing mechanisms and importance of uniformity of structure are deliberated.

Keywords: well-defined macromolecules; sequence-defined macromolecules; sequence-defined polymers; conjugated oligomers; oligo(arylene ethynylene)s; biosensors; sensors; process monitoring

1. Introduction

Nowadays, facing the development of precise polymer chemistry, in particular new synthetic methods that allow for monomer sequence control we are looking for new areas of application of macromolecules where the sequence matters. To design new applications of macromolecules the sequence–property relationship has to be well understood. Sensing and process monitoring are expanding areas where the structure of macromolecules and the sequence of monomers became a crucial parameter to achieve specificity and selectivity of the detection and bioprocess monitoring.

The monitoring of bioprocesses in an organism is performed by cascade communication between the network of biomolecules [1]. Biological components often react very sensitively to environmental changes (e.g., pH, temperature, nutrients), which may result in adverse effects on the activity of the cells or the reproducibility of the process. Uniform, sequence-defined macromolecules such as proteins and DNA are key features in the regulation of biological processes. The well-defined and sequence-controlled structures of those biomolecules enable precise recognition of specific molecular patterns or environmental changes (e.g., temperature, pH) to regulate the cascade events in the living organisms. The monomer sequence, for instance, amino acids in proteins or nucleotides in DNA,

determines functions and is responsible for regulation of thousands of cascade events in our body. The whole mammalian immune system relies on a large array of nucleic acid sensors [2,3].

The precision of the primary structure is also very important in man-made (bio)sensor systems based on conjugated macromolecules [4]. Over the last years, the synthetic strategies leading to well/sequence-defined macromolecules, that enable better control of the properties of resulting materials, were developed [5]. The monomer composition [6–19], sequence [4,6,12,19], and the oligomer length [6,9] are parameters that influence the energy levels of HOMO and LUMO orbitals in conjugated molecules. The structure indicates the energy gap between HOMO and LUMO, absorption, and emission properties in conjugated systems [6,19]. Even a slight modification of oligomer structure, e.g., in the side [20] or end groups [21,22], can affect its optoelectronic properties and influence sensing.

Conjugated macromolecules, due to their excellent optoelectronic properties, found great use in the construction of different types of sensors [23–25], e.g., monitoring of enzymatic activity [26], chirality sensors [27], protein sensing [28], material self-healing [29], diagnosis and drug discovery [25], biosensing and therapeutics [30]. The π-conjugated structure, allowing communication between monomers in molecules backbone, is responsible for excellent optoelectronic properties susceptible to environmental changes. The signal can be revealed in one or more dimensions [24] that induce selectivity of the read-out, e.g., chemical nose approach [25,31]. Multidimensional sensor response delivered by multiple sensor elements can selectively interact with the sample and produce a distinct pattern of response enabling specific identification of target components.

Among conjugated macromolecules, oligo(arylene ethynylene)s (OArEs) have gained considerable attention due to their excellent optoelectronic properties and emerging applications [32–35]. The current synthesis methods provide access to uniform OArEs of precise length and full sequence control [6,12,36]. OArEs are an important class of sensory materials [26,30,37–40]. OArEs sensors can be used in organic solvents as well as in the aqueous environment or as solid films. Their sensing mechanism usually takes advantage of their fluorescence properties, but not exclusively.

This review aims to summarize the examples of linear oligo(arylene ethynylene)s applied in sensing and to discuss their relevance and perspectives. Our study highlights the importance of adjustment and manipulation of their sequence and length to improve the performance of oligomer-based fluorescent sensors. The OArEs sensors in solution and solid films are discussed in the context of their applications in detection and process monitoring. The examples of oligomers that change properties upon the presence of a particular analyte or environmental changes are also included. Here, we focused on well-defined, uniform oligomers built from at least three arylene units connected via ethynylene linkage.

2. Synthesis of Well-Defined Conjugated Macromolecules

The synthetic strategies leading to uniform macromolecules that enable control over the monomer sequence have been introduced to polymer science during the last decades [41–43]. The nature-inspired need of defined macromolecular structures was a driving force to develop new synthetic methodologies, that combine current achievements of polymer chemistry, organic synthesis, and biochemistry to develop methods yielding uniform, sequence-defined macromolecules (Figure 1) [41,42,44,45].

In general, discrete macromolecules can be accessed by iterative synthesis. In principle, the synthesis relay on the stepwise attachment of protected monomers followed by deprotection. These two steps are repeated cyclically until the desired molecule is obtained. When the monomers are equipped with orthogonal functional groups there is no need for use of protecting groups [46,47]. Three main approaches can be distinguished: classical solution synthesis (Figure 1b), synthesis using a soluble polymer as a support (Figure 1c), or solid-phase synthesis (Figure 1d) [48]. The syntheses performed by classical organic chemistry methods are associated with cumbersome purification after each step. The use of polymeric supports in a soluble [6] or a solid phase [49] significantly simplifies the purification process.

In iterative synthesis it is very important to achieve high stepwise yields. The physical limitation of iterative synthesis is stepwise yield that determines possible length of macromolecules. The total

yield equals the product of actual step yield multiplying and, thus its value decreases dramatically with the number of steps, according to the formula:

$$Y_{total}[\%] = \prod_{i=1}^{n}\left(\frac{Y_n}{Y_{nth}} \times 100\right) \tag{1}$$

where: n—number of steps, Y_n—actual yield of step n [g], Y_{nth}—theoretical yield of step n expressed in mass units.

The Y_{total} drops dramatically with the number of steps. For example, if the stepwise yield Y_n will be 95%, after 50 steps total yield will be only 7%.
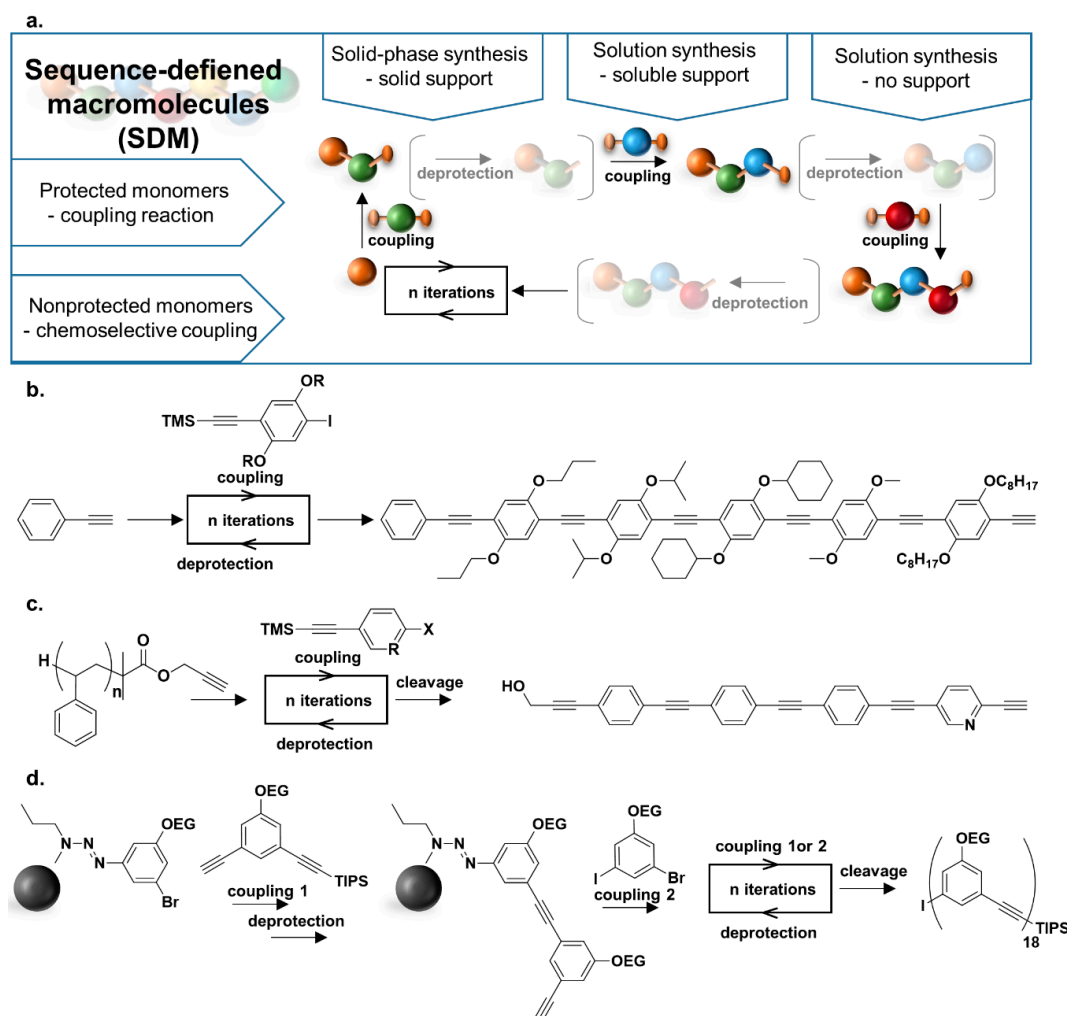

Figure 1. (**a**) The main approaches for the synthesis of sequence-defined conjugated macromolecules. Sequence-defined macromolecules can be obtained by multistep-growth synthesis using three main approaches: solid-phase synthesis, synthesis on soluble support, or solution synthesis. The monomers are used in a protected form that demands performance of the deprotection step after each coupling or by chemoselective reactions where monomers are equipped with orthogonal functional groups. The examples are of (**b**) solution synthesis [42], (**c**) synthesis on soluble support [6], and (**d**) solid-phase synthesis [11].

To obtain discrete conjugated oligomers (COs) based on oligo(arylene ethynylene)s skeleton, several stepwise synthetic strategies have been developed [42,50]. Usually, the oligomers are obtained by iterative solution synthesis that involves protected monomers. Due to poor solubility of arylene ethynylene oligomers they are usually synthesized from monomers functionalized by solubilizing

substituents. Oligomers are produced by successive coupling and deprotection steps that are repeated in the cycle until the preferred macromolecule is obtained [8,9,11,51–53]. An interesting alternative to classical solution-phase synthesis is the use of soluble or solid supports [7,10], in particular for longer oligomers synthesis. Those approaches significantly simplify purification after each step. The synthesis can be facilitated by divergent/convergent approaches [54] of bidirectional growth [55].

For example, the group of M.A.R. Meier established a solution synthesis protocol for sequence-ordered, uniform pentamers built from five different monomers [12]. The oligomers were synthesized by Sonogashira cross-coupling reaction followed by deprotection (Figure 1b). The photophysical properties of the monodisperse oligomers differed only slightly, but the sequence had an impact on their thermal properties and the hydrodynamic volume.

Oligo(arylene ethynylene)s without solubilizing substituents can be obtained by a soluble-support approach. An interesting example of the polystyrene-tethered synthesis of uniform and sequence-defined oligomers without solubilizing substituents was reported by R. Szweda et al. [6]. The use of an ATRP-made, tailored polystyrene support enabled the synthesis of OArEs containing sequence ordered pyridine and benzene units. For oligomer synthesis, Sonogashira cross-coupling reaction was used (Figure 1c). The use of the soluble support approach gave access to the unsubstituted oligomers that are inaccessible using other methods due to their limited solubility. The UV and fluorescent properties were changing with the oligomer length and composition.

The solid-phase synthesis of oligo(phenylene ethylene)s (OPEs) was reported by the group of J. M. Tour [9]. The synthesis of 16-units oligo(phenylene ethylene)s was demonstrated [9]. The authors applied an iterative divergent/convergent approach on Merrifield resin leading to oligo(2-alkyl-1,4-phenylene ethynylene)s. At each stage of the iteration, the length of the oligomer doubled. Another example of solid-phase synthesis leading to oligomers of 18 repeating units was developed by J. Moore [11]. In this approach, the monoprotected bisethynylarene and a 3-bromo-5-iodo arene monomers bearing orthogonal reactivity were used.

Alternatively, the discrete conjugated macromolecules can be obtained by purification of oligomers mixtures e.g., using reverse-phase chromatography [56] or automated flash chromatography [19] as demonstrated by the group of C. J. Hawker. The automated flash chromatography is an efficient separation method and can be used for the separation of thiophene oligomers of 2–14 units in grams scale [19].

Other methods often employed for the synthesis of COs as step-growth polymerization lead to mixtures of products of dispersity often higher than 1.2 [57]. Dispersity polymers consist of a mixture of structures which has a significant impact on the properties and optical behavior that may influence their sensing performance [58–60]. Moreover, the polymerization technique is not easily reproducible and in the context of sensor application that might be a crucial factor to obtain the same properties of materials. The resulting polymer even in the best-controlled conditions does not consist of uniform macromolecules. It is unlikely to obtain exactly the same mixture of macromolecules in two different polymerization processes.

Although lots of effort has been made, all of the existing methods show many limitations. The usual problems are low yields, limited molar mass (chain length), small synthesis scale, high synthesis cost, time, and labor consumption, etc. In the context of applications, those problems pose new challenges to the chemists to optimize the synthetic strategies, that will overcome existing limitations and enable further development of the field.

3. Macromolecular Conjugated Sensor Probes

Sequence-defined, uniform macromolecules based on linear oligo(arylene ethynylene)s backbone have been used in different types of sensors that can be classified into two main approaches: (i) solution probes, where oligomers are dissolved in a medium (Section 3.1) and (ii) solid-phase probes (Section 3.2), where oligomers are used as films or they are immobilized on a solid support. In the solution phase, we can distinguish two main sensor categories: classical OArEs (Section 3.1.1) and oligo(arylene ethynylene) electrolytes (Section 3.1.2), that possess ionic side-chains or end groups and exhibit water solubility. In this review, the compounds were divided according to the applied approach.

The oligo(arylene ethynylene)-based sensors can be also categorized according to the type of signal used in sensing, e.g., fluorescence, electrochemical, UV-vis, circularly polarized light (CD). Among the typical detection methods, the most popular is based on fluorescence that takes advantage of excellent optoelectronic properties of OArEs.

The sensing properties of OArEs strongly depends on their structure and chosen monomers. It was demonstrated that certain oligomers have specific structures and can selectively respond to the presence of particular species, e.g., selective detection of fibrillar and prefibrillar amyloid protein aggregates [61]. Sensing can be influenced even by little structural changes like oligomers length and monomer composition. In the following sections, the examples presenting the influence of structural factors on detection efficiency are discussed.

The examples of linear, discrete oligo(arylene ethynylene)s applied in sensing for detection and process monitoring are listed in Table 1. The oligomers that change properties upon the presence of a particular analyte or environmental changes are also included.

Table 1. Oligo(arylene ethynylene)s applied in sensing.

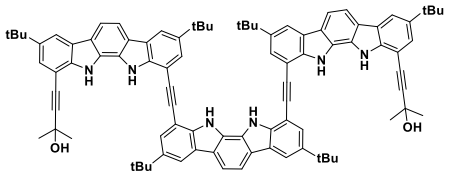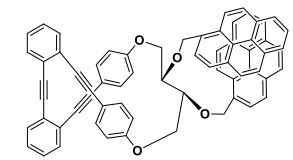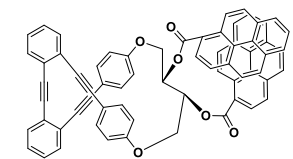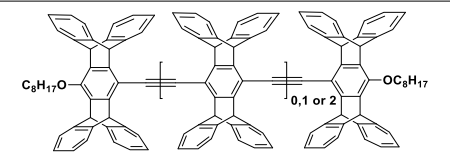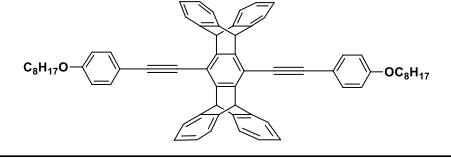| No.	OArEs Structures	Sensed Species (Potential Application)	Solvent/Medium (Concentration Range/LOD)	Sensing Mechanism	Detection Method	Ref.
		Oligo(phenylene ethynylene) in solutions				
1		D-fructose (fluorescent saccharide sensors)	Aqueous buffer pH 8.21 (D-fructose - 85-390 mM)	Reversible and pH-dependent complexation of phenylboronic acid with saccharides	FL	[38]
2		Octyl β-D-glucopyranoside	Dichloromethane and chloroform	Dynamic transformation between CD-silent dimer and CD-active helical oligomer-saccharide	CD, ^{1}H NMR	[62]
3		Cysteine (fluorescent chemical sensor for cysteine)	THF, THF/water (1:1, *v/v*) (1.0–10.0 μM)	Fluorescence quenching by blocking the photo-induced electron PET mechanism by free electron pair at N atom in Cys	FL	[63]
4		Enantioselective sensing of carboxylic acids, e.g., non-racemic tartaric acid (chiroptical sensing of carboxylic acids)	Chloroform (0.2 μM or 0.8 mM)	Chiroptical signals induced upon hydrogen bonding between urea protons and carboxylate groups in analytes	CD	[64]
5		Enantioselective sensing of carboxylic acids, e.g., non-racemic tartaric acid (chiroptical sensing of carboxylic acids)	Chloroform (0.2 μM or 0.8 mM)	Chiroptical signals induced upon hydrogen bonding between urea protons and carboxylate groups in analytes	CD	[64]

Table 1. *Cont.*

No.	OArEs Structures	Sensed Species (Potential Application)	Solvent/Medium (Concentration Range/LOD)	Sensing Mechanism	Detection Method	Ref.
6		Chiral organic ions, i.e., camphorsulfonates, adenosine 3′,5′-cyclic monophosphate (cyclic monophosphate chirality sensors)	CH_2Cl_2, MeOH/CH_2Cl_2 (1%, *v/v*) (1 mg/mL)	CD signal controlled/switchable through acid-base chemistry	CD	[65]
7		Silver (I) compounds: $AgBF_4$	CH_2Cl_2 or 95:5 mixture of CH_2Cl_2/acetone (0-2.5×10^{-4} M)	Organic monomolecular emitter which behaves as a circularly polarized luminescence (CPL)-based ratiometric probe	CD, FL	[66]
8		Silver (I) compounds: $AgBF_4$	CH_2Cl_2 or 95:5 mixture of CH_2Cl_2/acetone (0-2.5×10^{-4} M)	Organic monomolecular emitter which behaves as a circularly polarized luminescence (CPL)-based ratiometric probe	CD, FL	[66]
9		Temperature (fluorescent thermosensors)	$CHCl_3$; 2-methyltetrahydrofuran (80 to 320 K)	Change of the twist angles in the π-conjugated backbones depending on the temperature	FL	[67]
10		Temperature (fluorescent thermosensors)	$CHCl_3$; 2-methyltetrahydrofuran (80 to 320 K)	Change of the twist angles in the π-conjugated backbones depending on the temperature	FL	[67]

Table 1. *Cont.*

No.	OArEs Structures	Sensed Species (Potential Application)	Solvent/Medium (Concentration Range/LOD)	Sensing Mechanism	Detection Method	Ref.
11		Scratch healing efficiency in mussel-inspired polymer (monitoring of thermally triggered self-healing systems)	Air; temperature treatment at 60 °C	Reversible Zn−histidine interactions	FL, CLSM	[29]
Oligo(phenylene ethynylene)s electrolytes						
12		Methyl viologen (MV^{2+}), 3,3'-diethyloxacarbocyanine iodide (DOC) (optical materials in chemo- and biodetection)	Water pH 8 (MV^{2+} 0.01–0.3 µM; DOC 0.02–5 mM)	Amplified fluorescence quenching due to ion pairing between the oligomer and the quencher cation	FL, UV-vis	[68]
13		Ca^{2+}	Water pH 8 (0.02–10 mM)	Fluorescence shift	FL, UV-vis	[68]
14		bacteria: *Amycolatopsis azurea*, *Amycolatopsis orientalis* subsp. *lurida*, *Bacillus lichenformis*, *Bacillus subtilis*, *Escherichia coli* (BL21(DE3)), *Escherichia coli* (*E. coli* (DH5α)), *Escherichia coli* (*E. coli* (XL1 Blue)), *Lactococcus lactis*, *Lactococcus plantarum*, *Pseudomonas putida*, *Streptomyces coelicolor*, and *Streptomyces griseus* (efficient identification of bacteria)	5 mM phosphate buffer (pH 7.4); (OD$_{600}$ = 1.0)	Fluorescence recovery by replacement of conjugated polymers coupled on gold nanoparticles with bacteria	FL	[69]
15		4-nitrophenyl phosphate, bis(cyclohexylammonium) salt hydrate (NPP), disodium hydrogen phosphate (DHP), 9,10-anthraquinone-2,6-disulfonic acid disodium salt (AQS) (optoelectronic sensor devices)	Water, pH 7.0 (DHP < 0.25 mM, AQS 3.2 µM, NPP 10 µM)	Quenching effect due to formation of non-emissive aggregates	FL, UV-vis	[70]

Table 1. *Cont.*
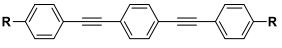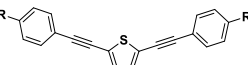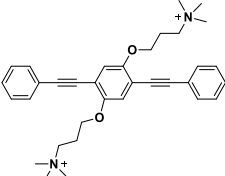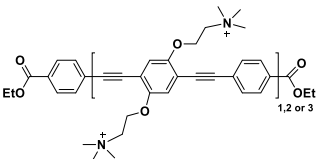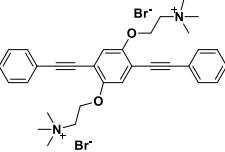
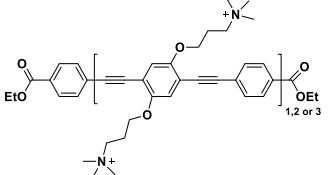| No.	OArEs Structures	Sensed Species (Potential Application)	Solvent/Medium (Concentration Range/LOD)	Sensing Mechanism	Detection Method	Ref.
16	R = OCH₂CH₂N⁺(CH₃)₃, OCH₂CH₂CH₂N⁺(CH₃)₃ or OCH₂CH₂CH₂SO₃⁻	Light-activated biocides against *Escherichia coli*, *Staphylococcus epidermidis*, and *Staphylococcus aureus*	0.85% NaCl in water	Under UV the conjugate photosensitize the generation of singlet oxygen which triggers the cytotoxicity	FL	[35]
17	R = OCH₂CH₂CH₂N⁺(CH₃)₃	Light-activated biocides against *Escherichia coli*, *Staphylococcus epidermidis*, and *Staphylococcus aureus*	0.85% NaCl in water	Under UV the conjugate photosensitize the generation of singlet oxygen which triggers the cytotoxicity	FL	[35]
18		Oxygen sensor for photosplitting of water	Water, argon-degassed water	Photoaddition of water across triple bond of ethynyl group in absence of oxygen, the addition of singlet-oxygen across a triple bond in presence of oxygen; formation of phenols via cleavage of alkoxy side chains in both cases	UV-vis, MS	[71]
19	1,2 or 3	Sodium dodecyl sulfate (SDS), carboxymethyl amylose (CMA), and carboxymethyl cellulose (CMeC)	Water, deuterium oxide (50 μM)	Fluorescence quenching by water; fluorescence enhancement due to formation of oligomer-surfactant complex	FL, UV-vis	[72]
20		4-nitrophenyl phosphate, bis(cyclohexylammonium) salt hydrate (NPP), 9,10-anthraquinone-2,6-disulfonic acid disodium salt (AQS) (optoelectronic sensor devices)	Water, pH 7.0 (AQS 6.1 μM, NPP 23 μM)	Strong fluorescence quenching in the presence of electron deficient species	FL, UV-vis	[70]

Table 1. *Cont.*

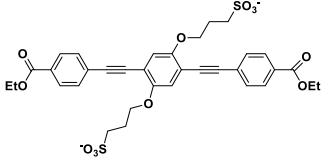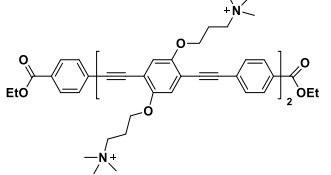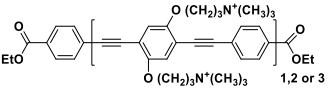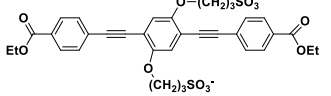| No.	OArEs Structures	Sensed Species (Potential Application)	Solvent/Medium (Concentration Range/LOD)	Sensing Mechanism	Detection Method	Ref.
21		Fibril formation from native hen egg white lysozyme (HEWL)	10 mM citrate buffer in water (pH 3)	Significant fluorescence enhancement in solution with HEWL amyloids	FL, CD	[73]
22		Amyloid protein aggregates Aβ40	pH 8.0 Tris (0.52 μM) pH 7.4 PB (0.48 μM)	Aggregate-specific binding inducing fluorescence turn on	FL	[61]
23		Amyloid protein aggregates Aβ40	pH 8.0 Tris (0.45 μM) pH 7.4 PB (0.24 μM)	Aggregate-specific binding inducing fluorescence turn on	FL	[61]
24		Activity of phospholipases (type A2, A1, C) and acetylcholinesterase (sensors of enzymes as biomarkers for pollution or disease)	Water, pH 7.5	Formation of molecular aggregates or conformational changes leading to change of photochemical properties	FL, UV-vis	[74]
25		Activity of phospholipases (type A2, A1, C) and acetylcholinesterase (sensors of enzymes as biomarkers for pollution or disease)	Water, pH 7.5	Formation of molecular aggregates or conformational changes leading to change of photochemical properties	FL, UV-vis	[74]

Table 1. *Cont.*
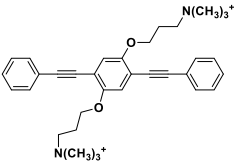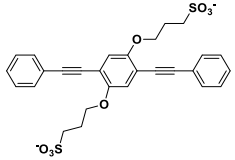
No.	OArEs Structures	Sensed Species (Potential Application)	Solvent/Medium (Concentration Range/LOD)	Sensing Mechanism	Detection Method	Ref.
26		Presented on the example of surfactants SDS and TTAB	Water	Formation of aggregates with strongly red-shifted absorbance	FL, UV-vis	[75]
27		Presented on the example of surfactants SDS and TTAB	Water	Formation of aggregates with strongly red-shifted absorbance	FL, UV-vis	[75]
28		Presented on the example of surfactants SDS and TTAB	Water (TTAB 0–200 μM, SDS 0–30 μM)	Fluorescence loss resulting from rapid internal conversion between singlet states	FL, UV-vis	[75]
29		Presented on the example of surfactants SDS and TTAB	Water (TTAB 0–200 μM, SDS 0–30 μM)	Fluorescence loss resulting from rapid internal conversion between singlet states	FL, UV-vis	[75]
30		Cationic surfactant cetyl trimethylammonium bromide (CTAB) (theranostic agent e.g., amyloid diseases)	Water (0–1500 μM)	Under UV the conjugate photosensitize the generation of singlet oxygen which triggers the cytotoxicity	FL, UV-vis	[76]
31		Anionic biomacromolecules; anionic biopolymer carboxymethylcellulose (CMC)	Water (0–42 μM)	strong spectral red shifts in both absorption and fluorescence coupled with the increase in fluorescence efficiency upon complexation with CMC	FL, UV-vis	[77]

Table 1. *Cont.*

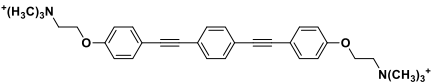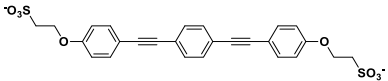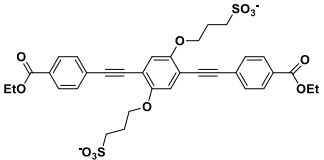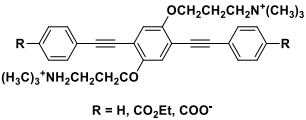| No.	OArEs Structures	Sensed Species (Potential Application)	Solvent/Medium (Concentration Range/LOD)	Sensing Mechanism	Detection Method	Ref.
32		Anionic biomacromolecules; presented the example of carboxymethylcellulose (CMC), carboxymethylamylose (CMA) and synthetic Laponite clay	Water (CMC 0–50 µM, CMA 0–0.28 µM, Laponite 0–31 µg)	Strong spectral red shifts caused by effective increase in the conjugation length upon template-induced formation of linear J-dimers or possibly because of planarization	CD, FL, UV-vis	[78]
33		Amyloid protein aggregates; detergents (i.e., carboxymethyl amylose (CMA) and carboxymethyl cellulose (CMeC)); activity of phospholipases (PL A2, A1, C) and acetylcholinesterase; phospahatase/kinase)	Organic solvents (e.g., methanol); water	Red/blue shift in the emission spectrum on the interface between the oligo-electrolyte and the analyte; reversible fluorescence turn-on (phospahatase–kinase; LOD of 0.05 units/mL)	FL	[79]
34		Amyloid protein aggregates; detergents (i.e., carboxymethyl amylose (CMA) and carboxymethyl cellulose (CMeC)); activity of phospholipases (PL A2, A1, C) and acetylcholinesterase; phospahatase/kinase)	Organic solvents (e.g., methanol); water	Red/blue shift in the emission spectrum on the interface between the oligo-electrolyte and the analyte; reversible fluorescence turn-on (phospahatase–kinase; LOD of 0.05 units/mL)	FL	[79]
35		Signal dependent on polarity of solvents (tunable luminescent sensory materials)	CH_2Cl_2, THF, 2-methyltetrahydrofuran	Controllable integration of functionalized phosphorescent signaling units into well-defined conjugated materials	FL, UV-vis, TAS	[80]
Oligo(phenylene ethynylene)s films						
36		*Escherichia coli* bacteria (new family of sensitive and selective biochips to detect *E. coli*)	Sample in a culture medium, (LOD = 10^4 CFU/mL)	Staining of bacteria by conjugated polymers	LSCM, SPR	[81]
37		*Escherichia coli* bacteria (new family of sensitive and selective biochips to detect *E. coli*)	Sample in a culture medium, (LOD = 10^4 CFU/mL)	Staining of bacteria by conjugated polymers	LSCM, SPR	[81]

Table 1. *Cont.*
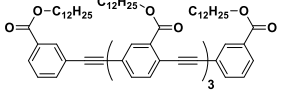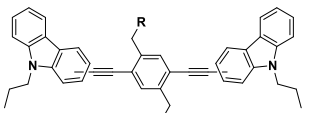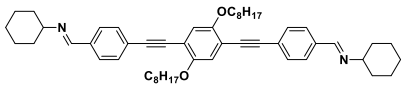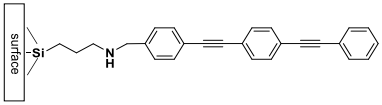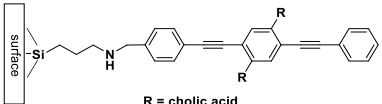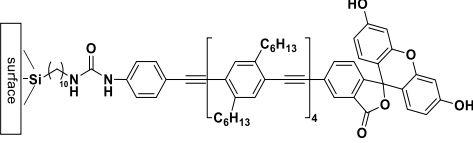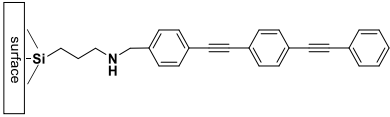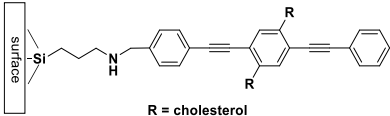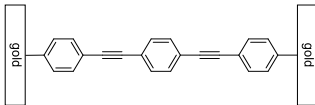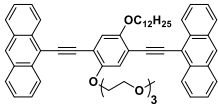
No.	OArEs Structures	Sensed Species (Potential Application)	Solvent/Medium (Concentration Range/LOD)	Sensing Mechanism	Detection Method	Ref.
38		Gram-positive *Bacillus subtilis* and Gram-negative *Escherichia coli*	Sample in miliQ water	Staining of bacteria by conjugated polymers	FL, LSCM, mRS,	[82]
39	R = 5,11,17,23-tetrakis(1,1-dimethylethyl)-25-(oxymethyl)-26,27,28-tripropyloxycalix[4]arene	Detection of high explosive materials and explosive markers: 2,4,6-trinitrotoluene (TNT) and 2,4-dinitrotoluene (DNT), nitromethane (NM), 2,3-dimethyl-2,3-dinitrobutane (DMNB)	Vapors in air	Amplified fluorescence detection response thanks to the establishment of a tridimensional network of strong π–π and CH–π interactions with electron-deficient guests developed near the transduction centers	FL	[83]
40		Detection of nitroaromatic explosives: trinitrotoluene (TNT), 2,4-dinitrotoluene (DNT),	Vapors in air, detection threshold—0.75 ppbv for TNT, 9 ppbv for DNT	In the presence of nitroaromatic explosives, conjugated fluorescent materials exhibit excellent fluorescence extinction properties due to a charge transfer mechanism	FL	[84]
41		Inorganic acids: HCl, H_2SO_4, HNO_3, H_3PO_4 (monomolecular layer chemistry-based fluorescent sensing films)	Acetone (5–40 µM)	Fluorescence quenching due to protonation of the imino group next to the conjugated segment	FL	[85]
42	R = cholic acid	Inorganic acids: HCl, H_2SO_4, HNO_3, H_3PO_4 (monomolecular layer chemistry-based fluorescent sensing films)	Acetone (5–40 µM)	Fluorescence quenching due to protonation of the imino group next to the conjugated segment	FL	[85]
43		pH (thin-film ratiometric chemosensors)	Water (pH 2–10)	Shift in the emission spectrum of fluorescein (formation of anionic isomers)	FL	[86]

Table 1. *Cont.*

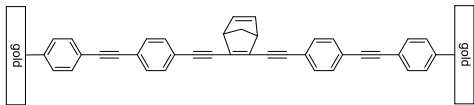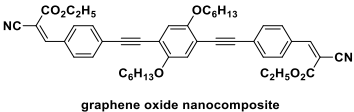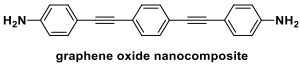| No.	OArEs Structures	Sensed Species (Potential Application)	Solvent/Medium (Concentration Range/LOD)	Sensing Mechanism	Detection Method	Ref.
44		2,4,6-trinitrophenol (PA), 2,4,6-trinitrotoluene (TNT), 2,4-dinitrotoluene (DNT), nitrobenzene (NB) (sensor for nitro compounds)	Water (PA, 0.2–5 μM; TNT, DNT, NB, 50 μM)	Reversible fluorescence quenching upon oligomer-analyte complex formation	FL	[87]
45	R = cholesterol	2,4,6-trinitrophenol (PA), 2,4,6-trinitrotoluene (TNT), 2,4-dinitrotoluene (DNT), nitrobenzene (NB) (sensor for nitro compounds)	Water (PA, 0.2–5 μM; TNT, DNT, NB, 50 μM)	Reversible fluorescence quenching upon oligomer-analyte complex formation	FL	[87]
46		H_2 (gas sensor for environmental monitoring)	-	Theoretical DFT-based model: adsorbed H_2 molecule significantly changes the characteristics of the current–voltage curve of the OPE molecular junction	CAL (DFT)	[88]
47		Data encoding	-	Electrically controllable local heating mechanism for the forward reaction and catalyzed by a single charge transferprocess for the reverse switching	CV	[89]
48	graphene oxide nanocomposite	Cysteine (fluorescent chemical sensor for cysteine)	THF (1.0–10.0 μM)	Fluorescent "turn-on" upon electrostatic attraction between carboxylic groups of oligomer and ammonium groups of Cys	FL	[63]
49	graphene oxide nanocomposite	Dopamine (electrochemical sensors)	Human serum in aqueous PBS (0.01–60 μM, LOD 5 nM)	Oxidation/reduction of dopamine on the film-modified electrode	CV	[90]
50		Perfluorocyclopent-1-ene-1,2-diyl)bis(5-methylthiophene-2-carbaldehyde (PBMC)	Solid state, xerogel, liquid, i.e., ethanol, water, methanol–water mixture (1:1)	Photoswitch based on pcFRET (on/off)	FL	[91]

Abbreviations: ^{1}H NMR—proton nuclear magnetic resonance spectroscopy, FL—fluorescence spectroscopy, CAL—calculations, CD—circular dichroism spectroscopy, CLSM—confocal laser scanning microscopy, CV—cyclic voltammetry, LOD—lower limit of detection, mRS—microRaman spectroscopy, MS—mass spectrometry, SPR—surface plasmon resonance, TAS—transient-absorption spectroscopy, THF—tetrahydrofuran, UV-vis—ultraviolet-visible spectroscopy.

3.1. Oligo(Arylene Ethynylene)s as Sensors Probes in Solution

3.1.1. Oligo(Arylene Ethynylene) Sensors

Oligo(arylene ethynylene)s have been used as sensors to detect different species e.g., chemicals [65], saccharides [38,62], amino acids [63], explosives [84], ions [66], and physical changes e.g., temperature [67] or solvent polarity [67]. OArEs were also used for process monitoring to track self-healing of polymers [29].

For example, the oligo(phenylene ethynylene)s foldamers with urea end-groups (Table 1, no. 4) were used for the detection of chiral carboxylic acids e.g., tartaric acid. [64] The stereodynamic oligomer-carboxylic acid complexes formed chiral structures easily detectable by CD measurements. It was demonstrated that the chiroptical signal could be used for quantitative analyses providing a fast and simple method for chirality sensing assays (Figure 2).
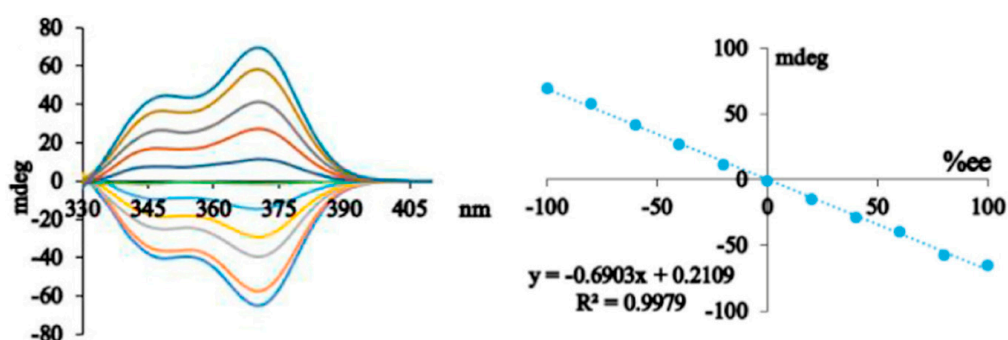
Figure 2. Circular dichroism (CD) spectra of the mixture obtained with oligo(phenylene ethynylene)s (Table 1, no. 4), Et$_3$N, and samples of tartaric acid and linear relationship between the CD amplitude at 370 nm and the sample enantiomeric excess. Reprinted from [64] with permission from Elsevier.

For instance, conjugated oligomers functionalized by boronic acid have been used as sensors to detect different saccharides: D-fructose, D-galactose, D-ribose, and D-glucose, in potassium phosphate buffer/DMSO (99/1, *v/v*) [38]. By the addition of saccharides, significant fluorescence enhancement was observed, and the response was different depending on saccharide. However, it was shown that the fluorescence response can be observed only for well-designed oligomer structures. The oligo(phenylene ethynylene)s with –OC$_{10}$H$_{21}$ side chains (Table 1, no. 1) and boronic acid groups attached via triazole linker were sensitive exclusively to fructose presence. It was found that the fluorescence response depends on supramolecular interactions between sensors and analyte molecules which are very structure dependent. This study highlighted the need for a specific design of oligomer fluorophore in the development of effective saccharide sensors.

Ortho-oligo(phenylene ethynylene)s (Table 1, no. 7, 8) were used as a circularly polarized luminescence probe for the detection of silver ions [66]. The enantiopure helical core has been prepared by a new macrocyclization reaction. The combination of such o-OPE helical skeleton and pyrene reporter units lead to two characteristic circularly polarized emission features. The intensity of the bands linearly corresponds with silver(I) concentration.

Interestingly, the temperature change that is a physical process can be followed by oligo(arylene ethynylene)s [67]. The acetylene-bridged pentiptycene (n = 2, 3, and 4) (Table 1, no. 9) and phenylene−pentiptycene−phenylene three-ring system (Table 1, no. 10) were evaluated as fluorescent temperature sensors. The trimer and tetramer showed a unique response to temperature and solvent polarity driven by intramolecular interactions (Figure 3). It was found that the twisted region of their rotational potentials occurs at the local energy minimum, and the distribution of rotational conformers is sensitive to the temperature and solvent polarity. Twisting of the π-conjugated backbones reflected in 40 nm blue-shifted fluorescence spectra. It was demonstrated that upon temperature change in the

range between 80 and 320 K, the fluorescence emission of acetylene-bridged pentiptycene tetramer shifted significantly. This property can be used for the development of low-temperature sensors.
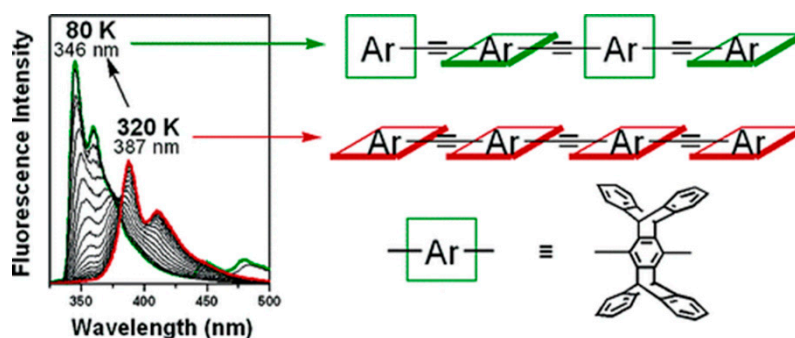
Figure 3. The change of conformation caused by temperature difference influence the fluorescence properties. Temperature dependence of fluorescence spectra (λ ex = 303 nm) of tetramer in methylotetrafuran at 20- and 10-K intervals, respectively, between 80 and 320 K. Reprinted with permission from [67]. Copyright 2006 American Chemical Society.

Recently it was demonstrated that oligo(arylene ethynylene)s (Table 1, no. 11) can be used as a fluorescent probe for monitoring of the self-healing process [29]. The OPE incorporated into a mussel-inspired scratch-healing polymer network helped to determine detailed depth- and time-dependent self-healing efficiency using confocal laser scanning microscopy (Figure 4). The damage of the network resulted in decreased fluorescence emission of polymer within the scratch. The mobility of the fluorescence marker is connected with the plasticity of the polymeric material, thus during scratch refilling, no independent migration of dye within the polymeric material was detected.

3.1.2. Oligo(Arylene Ethynylene) Electrolytes

Oligo(arylene ethynylene) electrolytes are very attractive macromolecules for application in sensing. As sensor probes, they combine the excellent fluorescence properties of a conjugated aryl-alkyne system with electrolyte advantages especially water solubility [35]. Due to the presence of ionic groups, these oligomers are very sensitive to the environment changes, e.g., ionic strength, pH, presence of ions, presence of electrolytes. The charged pendant groups can induce electrostatic interactions with oppositely charged (macro)molecules that reflect in fluorescence properties variation [37]. Moreover, the charges distributed along the oligomer molecules affect their aggregation thus they exhibit high fluorescence response to alterations of aggregates structure and conformational changes. Those changes caused by the presence of individual charged molecules may reveal a unique response in the photophysical properties of the conjugated chromophore. The resulting fluorescence quenching or enhanced emission can indicate presence of ions [70], oxygen [71], surfactants [70,72,75,79,92], detergents [76,79], MV^{2+} ions [68], solvent polarity [80], anionic biopolymer carboxymethylcellulose [77,78], biomolecules [93], and bacteria [69]. The oligomers were used for processes monitoring of e.g., amyloid formation [61,73], enzymatic activity [74], and photochemical reaction processes [71].
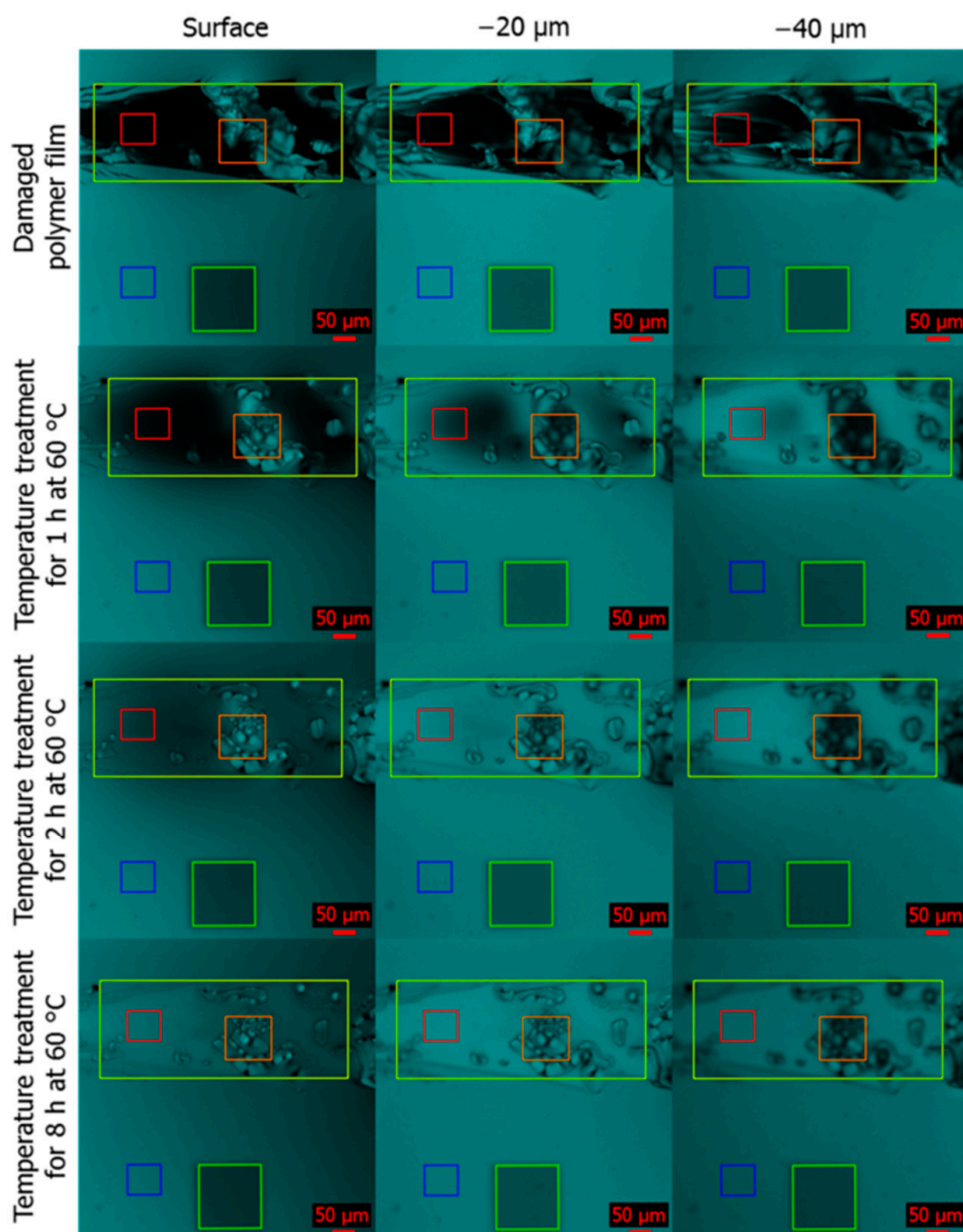
Figure 4. Time- and depth-dependent confocal laser scanning microscopy (CLSM) measurements in fluorescence mode (λ_{ex} = 405 nm) with the fluorescence channel (λem = 406–510 nm) monitoring thermally triggered self-healing procedure, in particular the virgin damaged cross-linked copolymer film, after 1, 2, and 8 h of thermal treatment at 60 °C: (red) homogeneous area within the scratch, (yellow) heterogeneous area covering the majority of the analyzed defect, (orange) specific area with residual removed film material, (blue) intact and undamaged reference area for each measurement, and (green) photo-bleached marker area. Reprinted with permission from [29]. Copyright 2018 American Chemical Society.

For instance, the oligo(p-phenylene ethynylene) electrolytes (OPE) were successfully applied to track amyloid formation [61,73]. Oligomers with ester terminal moieties and positively charged $-(CH_2)_3N(CH_3)^{3+}$ pendant groups of different length OPEn (n = 1, 2, and 3) (Table 1, no. 21) and OPE1 negatively charged with pendant $-(CH_2)_3SO^{3-}$ groups (Table 1, no. 22) were evaluated as probes for monitoring of the fibrillation process (Figure 5) [61,73]. The carboxyester terminal groups

of OPEs cause high fluorescence quenching due to the strong interactions with the solvent, on the other hand, the oligomers show strong fluorescence emission when in a water-poor environment. These environment-dependent fluorescence properties were used for the sensor design. It was demonstrated that positively charged OPEs used in 10:1 (protein:OPE) molar ratio are effective molecular taggants for selective sensing of the amyloid fibril of the model protein HEWL. Upon fibril formation, OPEs form clusters with the fibrils, where the carboxyester terminal groups are isolated from water. In a non-water environment, they form superluminescent chiral J aggregates [94] and significant fluorescence enhancement is observed (Figure 5). It was found that due to the energy transfer the excitation at 280 nm characteristic for HEWL results in the emission of OPE only in solutions containing OPEs and HEWL amyloids that indicate amyloid formation.
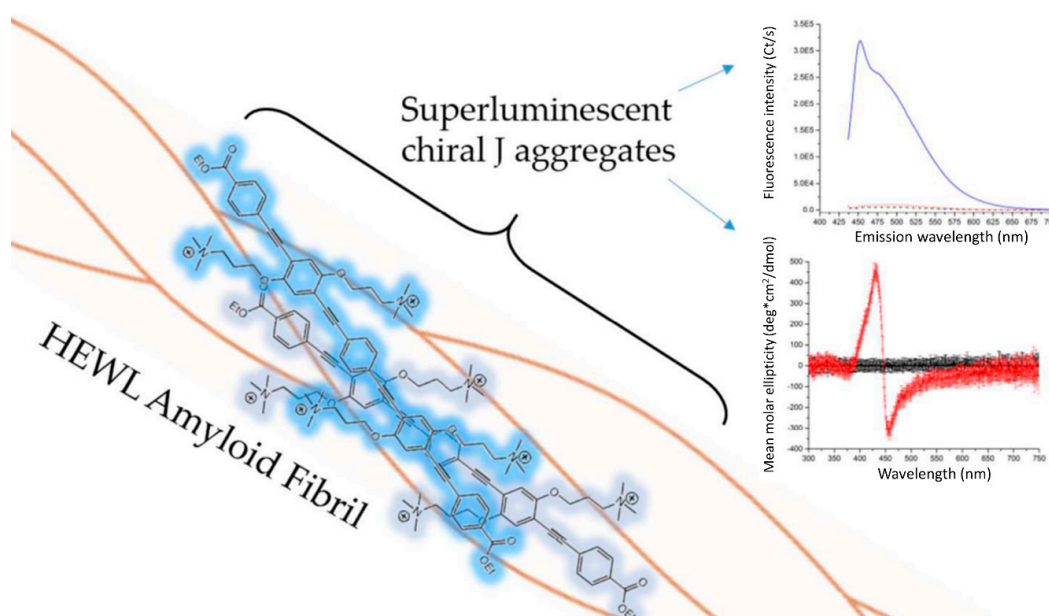
Figure 5. Oligo(p-phenylene ethynylene) (OPEs) electrolytes are forming specific chiral constructs together with amyloid fibrils. The construct exhibits enhanced fluorescence quenching and a unique CD signal. Circular dichroism spectra of OPE n = 3 (10 μM) in phosphate buffer with hen egg white lysozyme (HEWL) monomer (black trace) and with HEWL (10 μM) amyloid (red trace). Emission spectra of OPE n = 3 in phosphate buffer (PB, pH 7.4, 10 mM) alone (black long dashed line) with HEWL monomers (red short dashed line) and with HEWL amyloids (blue solid line), concentration: 500 nM, protein concentration: 5 μM monomer basis/0.25 mg/mL. Reprinted with permission from [73]. Copyright 2015 American Chemical Society.

p-Phenylene ethynylene oligomers can be also used for monitoring of enzymatic processes. Complexes of oligomers (Table, no. 24, 25) with enzyme substrates were successfully used to follow activity and inhibition of two biomarkers, phospholipase indicating heart and circulatory disease, and acetylcholinesterase for Alzheimer's diagnosis (Figure 6) [74]. In a buffer solution, oligomers form complexes with positively charged substrates e.g., 1,2-dilauroyl-sn-glycero-3-phosphoglycerol (DLPG) and lauroyl choline (LaCh). The DLPG-oligomer (Table, no. 24) complex upon phospholipases undergoes transformation due to the cleavage of DLPG phosphate bond that resulted in a swift of the fluorescence quenching. The aggregates of an anionic oligomer (Table, no. 25) with lauroyl choline were used as a sensor to detect the activity and inhibition of acetylcholinesterase.
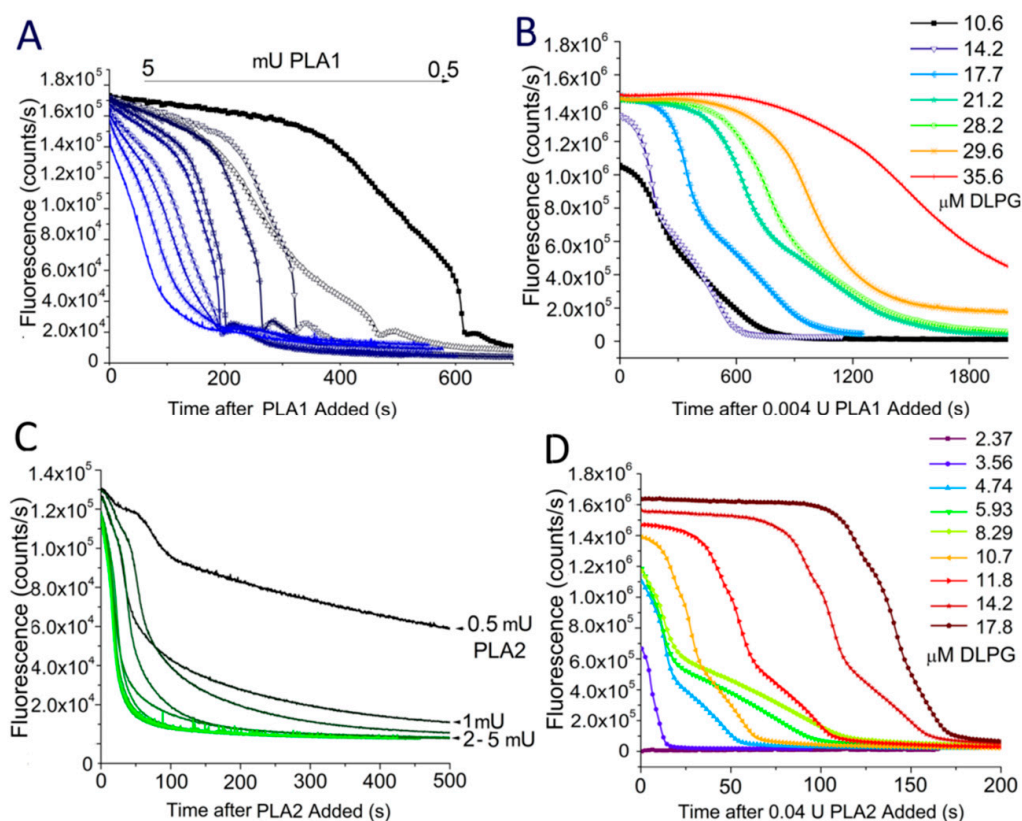
Figure 6. (**A**) Fluorescence of the oligomer/1,2-dilauroyl-sn-glycero-3-phosphoglycerol (DLPG) (Table 1, no. 24) aggregates over the course of Phospholipase A1 activity with 1.4 μMOPE and a DLPG concentration of 7.27 μM, with enzyme added ranging from 0.5 to 5 mU of Phospholipase A1. (**B**) A concentration of 1.4 μM of +2C with DLPG at a series of concentrations from 10.6 to 35.6 μM (7.5–25.4 DLPG:OPE ratio), followed by the addition of 4 mU of Phospholipase A1. (**C**) Fluorescence of the oligomer/DLPG aggregates over the course of Phospholipase A2 activity with 1.4 μM oligomer and a DLPG concentration of 7.27 μM, with enzyme added ranging from 0.5 to 5 mU of Phospholipase A2. (**D**) A concentration of 1.4 μM of +2C with DLPG at a series of concentrations from 2.37 to 17.8 μM (1.7–12.7 DLPG:oligomer ratio), followed by addition of 40 mU of Phospholipase A2. t = −1 s is the time of enzyme addition. Wavelength of excitation is 375 nm, emission is 440 nm. Reprinted with permission from [74]. Copyright 2015 American Chemical Society.

OArEs (Table 1, no. 18) can be used to monitor chemical processes, e.g., photolysis [71]. For example, the photo-induced degradation process of oligomer (Table 1, no. 18) occurred by three main routes: the photoprotonation of the triple bond followed by the addition of water, the addition of singlet oxygen across the triple-bond, and the cleavage of the quaternary ammonium side-chains. The degradation led to the formation of different products depending on the reaction atmosphere (argon or oxygen). All those structural changes reflected in fluorescence properties indicating the rate and mechanism of the degradation. Whenever the process was performed in the presence or absence of oxygen, different products of different fluorescence properties were formed. The dependence of fluorescence properties on the reaction atmosphere led to developing an oxygen-sensing methodology based on fluorescence read-out of OArE photo-degradation.

Constructs of oligo(phenylene ethynylene)s electrolyte and gold nanoparticles can be used for selective bacteria identification using the "chemical nose" sensing concept (Table 1, no. 14) [69]. In a solution, positively charged gold nanoparticles form complexes with negatively charged oligo(phenylene ethynylene)s, and oligomer fluorescence is quenched. In the presence of bacteria, some OPEs are released to the solution and fluorescence is restored as a consequence of the presence of free oligomers (Figure 7). The applied oligomer with branched oligo(ethylene glycol) side chain

reduces the non-specific interaction of oligomer and bacteria. Depending on bacteria the oligomer replacement is different which results in selective fluorescence response.
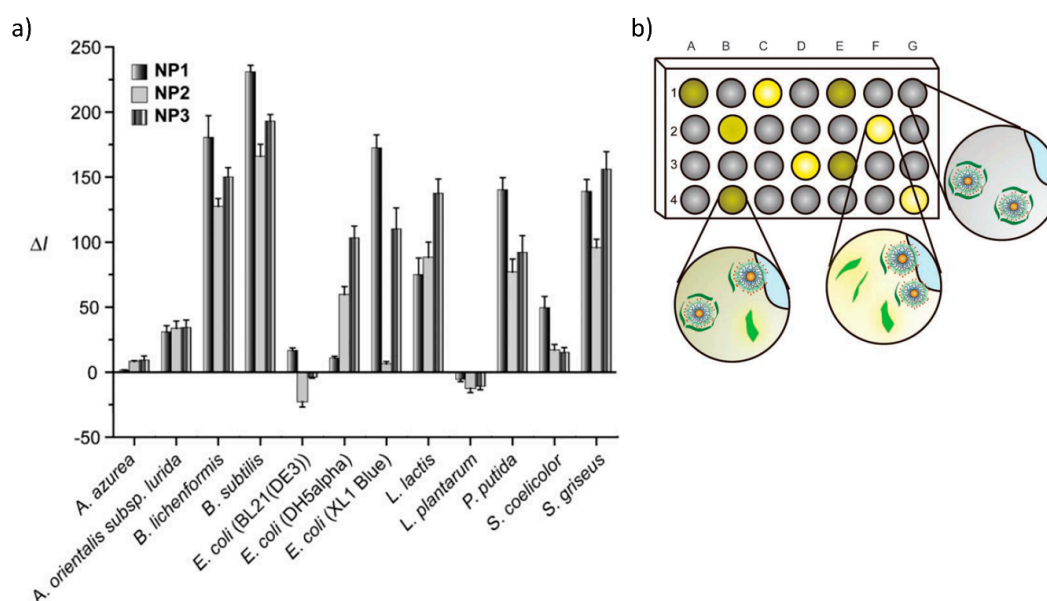
Figure 7. (**a**) Fluorescence intensity patterns of nanoparticle–oligomer (Table 1, no. 14) constructs in the presence of various bacteria strains. (**b**) The schematic presentation of sensor design. Bacteria interact with gold nanoparticle-oligomer construct and as oligomers macromolecules are released to the solution, fluorescence enhancement is observed. For each bacteria, interactions with nanoparticles are unique. In the figure, columns represent bacteria of different types, and rows represent the oligomer–nanoparticle constructs. Reprinted with permission from [69]. Copyright 2008 John Wiley and Sons.

The π-conjugated oligo(phenylene ethynylene) backbones with two negatively charged $-CH_2COO^-$ groups on each repeating unit and lengths of n = 5, 7, and 9 (Table 1, no. 13) were used to detect Ca^{2+} ions and quenching ionic agents [68]. In the presence of bivalent calcium ions, the oligomers aggregated causing fluorescence shift. The shift depended on oligomer length and for the shorter oligomers (n = 5, 7), the effects are less pronounced than for longer ones n = 9. This shift can be explained by the planarization of the phenylene ethynylene backbone and formation of "excimer-like" excited states, that are not observed in the absence of Cu^{2+} ions. The ligomers were also evaluated for fluorescence quenching in the presence of methyl viologen and 3,3'-diethyloxacarbocyanine–well-known fluorescence quenching agents. It was found that the quenching efficiency depends on oligomer length. Taken together, the elongation of oligomer increased the ionic charge of macromolecules that in presence of counter ions favor the formation of ordered and backbone-overlapped aggregates.

For example, while the fluorescence of cationic OPEs with amine end groups is quenched in water, the addition of a small amount of oppositely charged detergent, sodium dodecyl sulfate (SDS), causes a significant increase in the OPE fluorescence due to the formation of a complex (Table 1, no. 16, 17) [35]. These OPE-detergent complexes exhibited antimicrobial properties [95], which, in addition to the fluorescence emission during their formation, can be utilized for the development of multifunctional biosensors.

3.2. Oligo(Arylene Ethynylene) Sensor Films

Oligo(arylene ethynylene) films consist of packed macromolecules with π-conjugated backbone thus exhibit high fluorescence emission which can be altered upon binding of an analyte molecule. OArEs films are an excellent materials for detection of amino acids [63], bacteria [81,82], explosives [35,83,84,87], pH [86], inorganic acids [85], gas [88], digital information [89], or

chemicals [90,91]. Usually, the detection of an analyte is based on fluorescence changes, its enhancement or quenching upon binding of the sensed molecule. The OArEs films can be obtained by covalent immobilization e.g., reaction between an aldehyde and amine-functionalized surface [85,87], triethoxysilane group and glass [86], electrostatic binding [96], or drop-casting [90].

For instance, oligo(phenylene ethynylene)s bearing 4-aminophenyl-D-mannopyranoside groups (Table 1, no. 36, 37) in combination with laser scanning confocal microscopy have been used for the detection of *E. coli* bacteria [81]. Oligomer probes with two mannose groups enable discrimination between uropathogenic and the non-uropathogenic *E. coli* mutant. Moreover, the films of oligomer on aluminum support together with SPR allowed for quantitative biosensing of uropathogenic *E. coli* achieving a LOD of 10^4 CFU/mL. Those findings showed the direction towards robust biochips to detect bacteria.

For example, oligo(p-phenylene ethynylene) (Table 1, no. 44, 45) films have been examined in sensing of common explosive nitroaromatic compounds (NACs) i.e., 2,4,6-trinitrophenol (picric acid, PA), 2,4,6-trinitrotoluene (TNT), 2,4-dinitrotoluene (DNT), and nitrobenzene (NB) [87]. Interestingly, the film with cholesterol side groups (Table 1, no. 45) exhibited sensitivity to changes of water/THF solvents ratio (Figure 8a). In water, the film adapted a compacted structure causing a decrease in fluorescence intensity whereas in THF the chains attained extended conformation. In the presence of NACs molecules, complete fluorescence quenching was observed as the effect of the formation of nonfluorescent OPE-NACs complexes. This effect was not interfered by the presence of other compounds, including methanol, THF, toluene, dichloromethane, ammonia, HCl, NaOH, NaCl, copper salts, or seawater (Figure 8b). The experiments revealed that the cholesterol chains incorporated in the oligomer structure induced the sensitivity of the films towards the detected molecules by at least one order of magnitude. Thus, the films of oligo(p-phenylene ethynylene) with cholesterol groups can be used as an effective sensor for explosives.

Surface-immobilized monolayers of defined in length, short oligo(p-phenylene ethynylene) oligomers end-capped by fluorescein (Table 1, no. 43) have been used as narrow-range threshold fluorescent pH indicators (Figure 9a) [86]. At low pH, fluorescein was in its lactone form and the observed emission mostly originated from the oligomer. Upon pH increase fluorescein form change to anionic that favors electron delocalization with a respective decrease in HOMO-LUMO gap. A smaller energy gap facilitates the exciton migration that results in fluorescence enhancement. Moreover, an increase of pH causes a bathochromic shift of oligomer emission due to energy transfer from the oligomer backbone to fluorescein (Figure 9b). This unique pH-dependent response was observed only for oligomer-fluorescein dyad structures immobilized on the surface. The dyad structure was crucial for sensor selectivity. Experiments performed for immobilized fluorescein did not reveal such a selective sensor response. For comparison the same experiment was performed for dyad oligomers in solution, however, the fluorescence signal was much weaker in intensity and the pH validation range was significantly narrowed (pH 8 to 10).
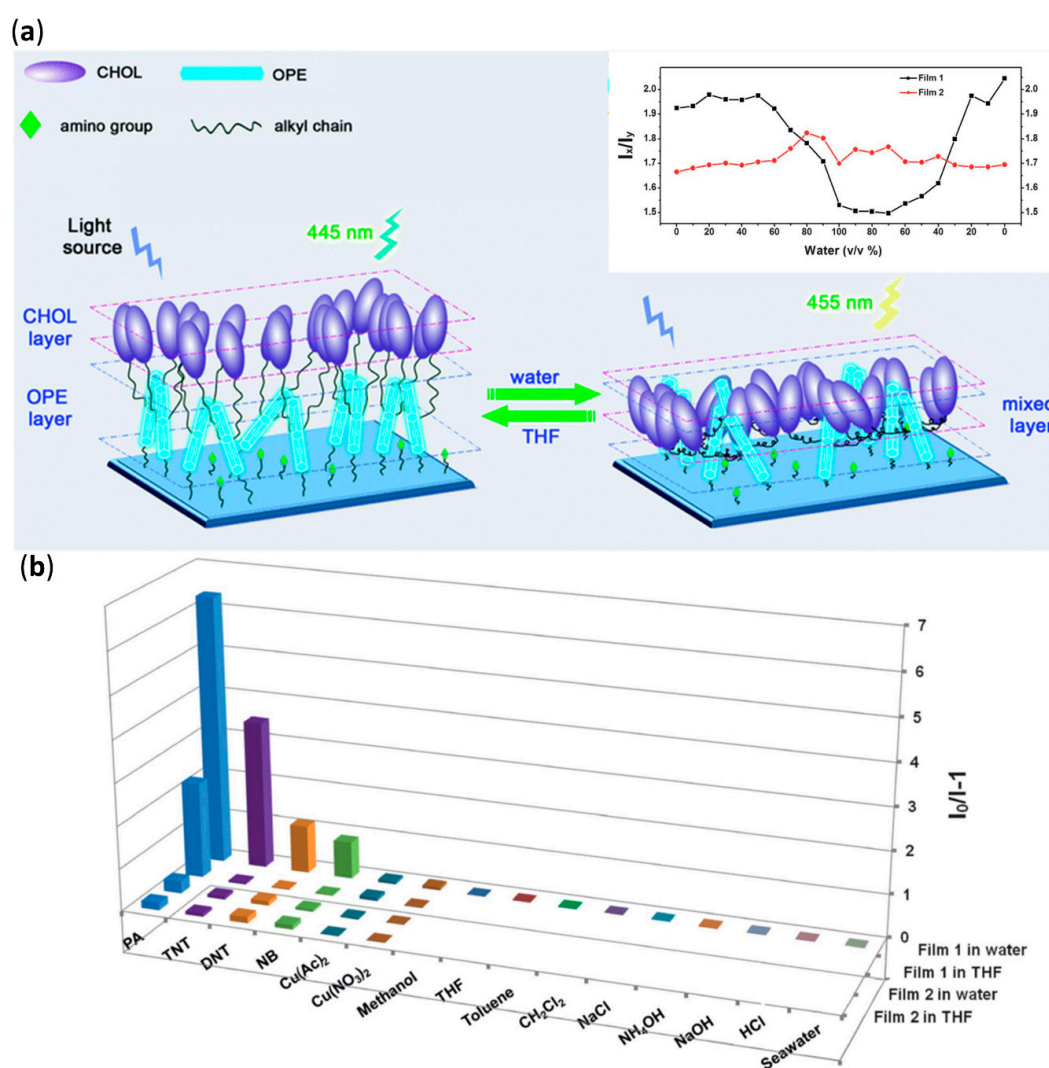
Figure 8. (**a**) The two states adopted by the oligomers containing cholesterol side chains (Table 1, no. 45) in water and tetrahydrofuran (THF), respectively. THF is a good solvent for oligomer and its cholesterol side chains and macromolecules in the film attain extended conformation. In contrast, water is a poor solvent for both the oligomer backbone and the side chains, thus the oligomer film is collapsed. Plots of the ratios of Ix/Iy of a given fluorescent film (Film 1-oligo(p-phenyleneethynylene) with cholesterol moieties and Film 2-pristin oligo(p-phenyleneethynylene)) against the compositions of the mixture solvents in which the fluorescence measurements were conducted (for Film 1 (Table 1, no. 45), λ_{em} = 445 nm, y λ_{ex} 500 nm; for Film 2 (Table 1, no. 44), λ_{em} 374 nm, λ_{ex} 420 nm). (**b**) Quenching efficiencies of various common explosive nitroaromatic compounds (NACs) on the fluorescence emission of Film 1 and Film 2 in water and THF, respectively, and the interferences of commonly found interferents in the sensing of Film 1 (concentration of NACs and interferents are 50 mM). Adapted from [87] with permission from The Royal Society of Chemistry.
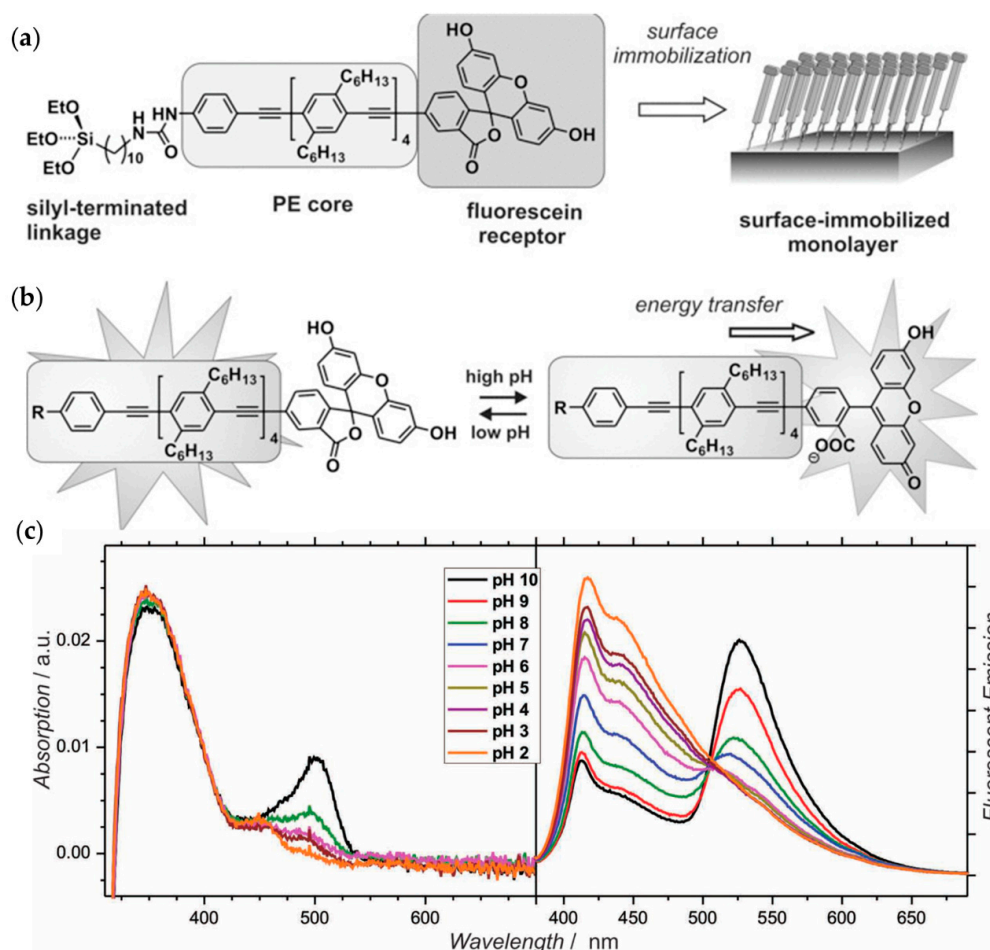
Figure 9. (**a**) Structure of the sensor and its assembly into a surface-immobilized monolayer. (**b**) The general principle of generating pH-dependent fluorescent response. (**c**) pH-dependent absorption (left) and fluorescence (right) spectra of monolayer fluorescein-oligomer film. Reprinted with permission from [86]. Copyright 2013 John Wiley and Sons.

Additionally, immobilized oligo(p-phenylene ethynylene) can act as chemosensors for the detection of polar species in an aprotic solvent. For example, a self-assembled monolayer of oligo(p-phenylene ethynylene) with cholic acid moieties (Table 1, no. 42) immobilized onto a glass slide, has been used as a sensor for trace amounts of inorganic acids, such as HCl, H_2SO_4, HNO_3, and H_3PO_4, in acetone medium [85]. The presence of a cholic acid unit induced the formation of hydrophobic pockets in the upper part of the layer (Figure 10a). This pocket containing imino group was able to trap ions that interacted with the imino groups. Basing on the comparative studies performed for different acids, it was revealed that for the anaerobic acids, the quenching efficiency depended on the size of the molecule and hydrogen bonds between the anions (Figure 10b). In other words, to observe efficient quenching the acid ions had to fit the cavity of the hydrophilic pocket. When chloride anion was trapped in the pocket the fluorescence quenching originated from the protonation of the imino group next to the phenylene ethynylene segment was observed.
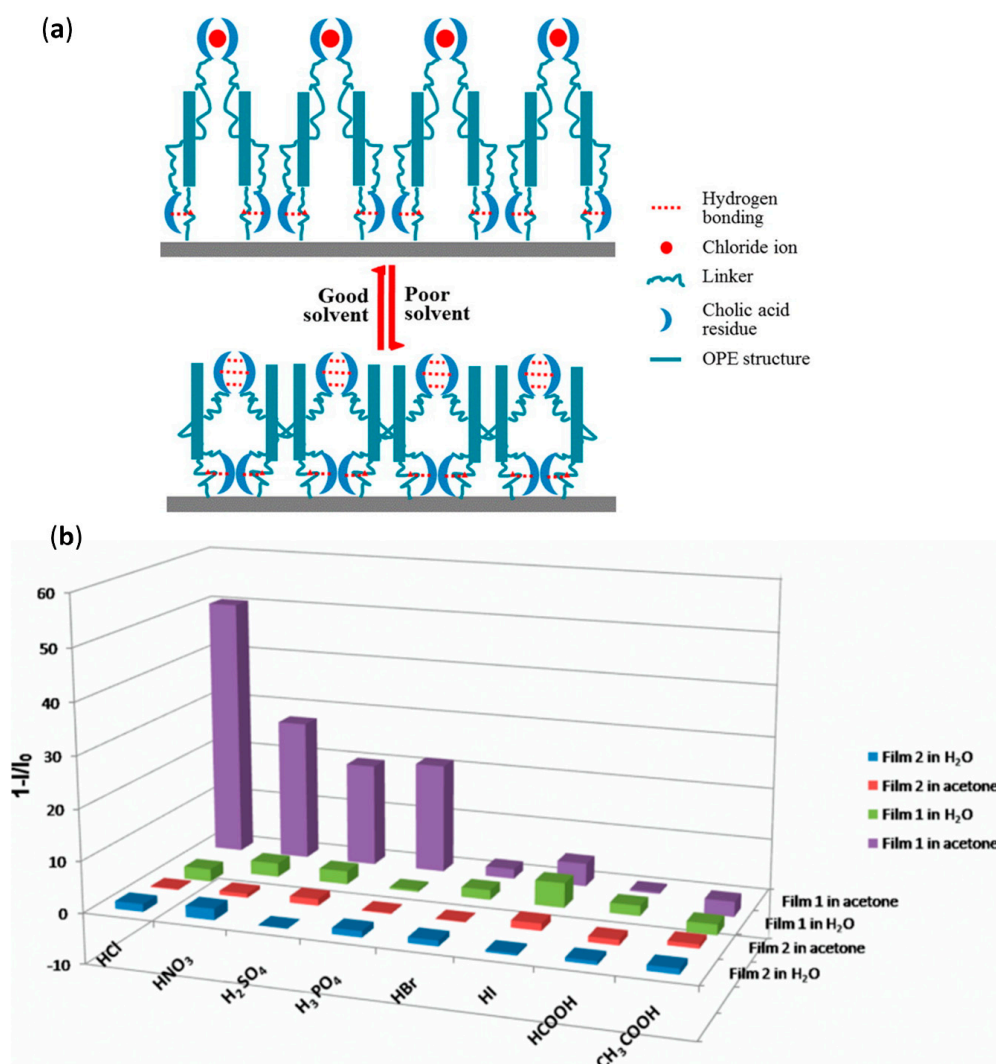
Figure 10. (**a**) Illustration of immobilized oligomer (Table 1, no. 42) conformations in different medium representing good (acetone as an example) or poor solvent (water, for example). In a good solvent, the hydrophilic pocket is formed as an upper layer of the film. (**b**) Quenching efficiencies of various acids to the fluorescence emission of Film 1-oligo(p-phenylene ethynylene) with cholic acid side chains (Table 1, no. 42) and Film 2-oligo(p-phenylene ethynylene) (Table 1, no. 41) in water and acetone, respectively (concentration of acids are 20 μM). Reprinted with permission from [85]. Copyright 2012 American Chemical Society.

Very sensitive sensor response can be achieved using electrochemical sensing methods. An electrochemical sensor based on an oligo(phenylene ethynylene) (Table 1, no. 49) and chemically reduced graphene oxide (rGO) nanocomposite was used for the quantification of dopamine (DA) [90]. This nanocomposite was synthesized by a simple ultrasonication method and then drop-casted onto a polished glassy carbon electrode and followed by casting of a Nafion ethanol solution (0.25 wt%). The formation of the oligomer nanocomposite was attributed to the π–π stacking interaction between the conjugated structure of oligo(phenylene ethynylene) and rGO as well as the electrostatic force between the amino group of oligomer and the carboxyl group on rGO. Anchoring of the oligomer changed the configuration of the multiple bonds so that a conjugated system represented a characteristic feature of conducting polymers. The developed sensor exhibited significantly enhanced electrocatalytic activity toward the oxidation of DA in a human serum PBS solution in the concentration range of 0.01–60 μM with LOD of 5 nM, a significantly lower value than those reported for the other DA sensors [97].

A chemical sensor based on GO-oligo(phenylene ethynylene) (Table 1, no. 48) nanocomposites was developed for amino acid detection [63]. The oligo(phenylene ethynylene) with cyanoacrylate groups in presence of cysteine residue change fluorescence properties. As a result of the interaction between oligomer and cysteine blue-shifted and decreased fluorescence emission was observed. For oligomer-GO nanocomposite the behavior was opposite and fluorescence enhancement occurred. The strong response of oligomer to cysteine can be used as a highly sensitive sensor.

Oligo(phenylene ethynylene)-based temperature sensors have been used to encode digital information [89]. The oligomers (Table 1, no. 47) were used as junctions between two Au electrodes (Figure 11a). Interestingly, during local temperature changes, the oligomers were able to change their structure between norbornadiene (NB)-state and quadricyclane (QC)-state (Figure 11d). The molecule states exhibited different conductance values that can be assigned to "1" and "0" digital symbols. The temperature-dependent conducting properties of oligomers could be used for local temperature monitoring. This system due to the clear response, translated into two states can be further exploited as a new approach for encoding digital information.
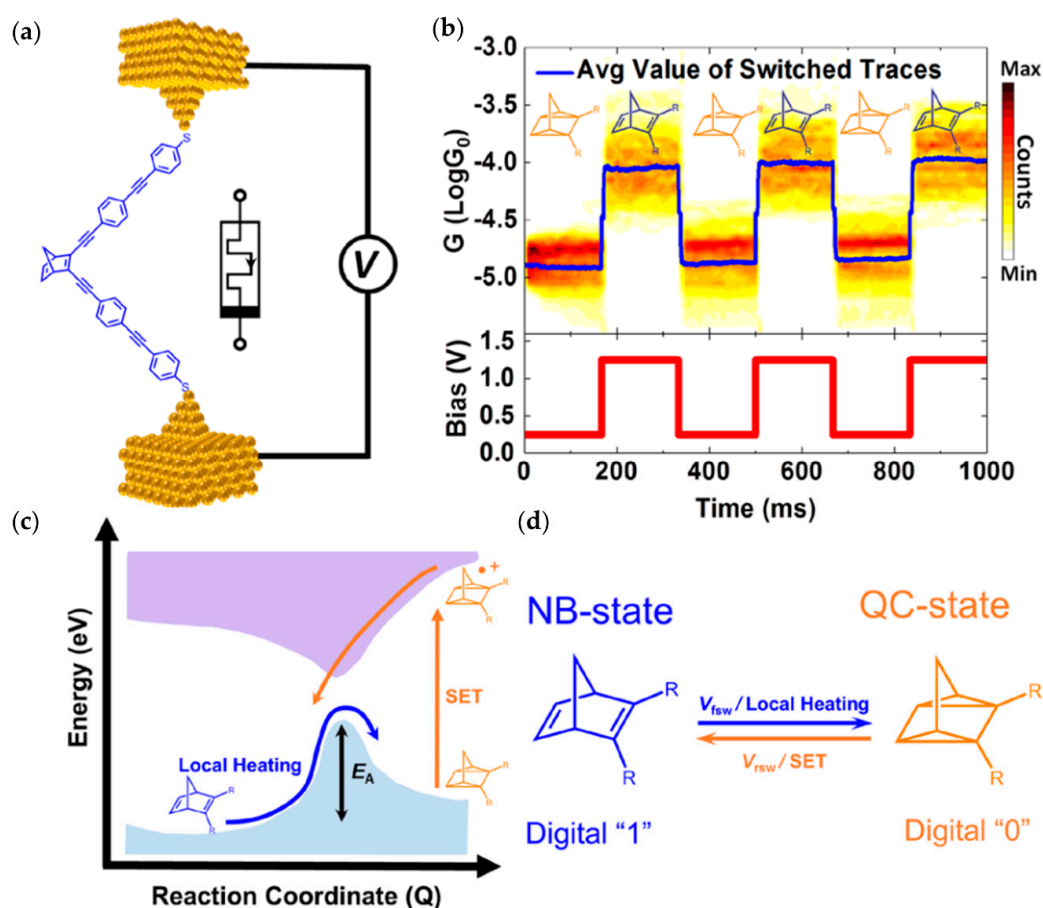
Figure 11. (**a**) Schematic of the molecular device with a modulating bias. (**b**) Reversible switching behavior of single-molecule devices and the applied waveform. (**c**) Energy landscape of isomerization processes. Blue and orange arrows indicate the electrically controlled forward and reverse switching processes, respectively. (**d**) Schematic describing the processes for controlling the norbornadiene (NB)-quadricyclane (QC) switching within a molecular junction (blue and orange arrows). The switching processes within a molecular junction are controlled in the forward direction (NB to QC) by electrically controlling the local temperature and in the reverse process (QC to NB) by catalyzing the reaction through a single electron transfer (SET) process. These two states possess different conductance values and can be used to encode digital information. Reprinted with permission from [89]. Copyright 2020 John Wiley and Sons.

4. Conclusions

Uniform, π-conjugated oligomers based on an arylene ethynylene core are attractive sensory materials. They can respond to the environment changes (polarity, temperature), presence of chemicals (amino acids, saccharides, ions), macromolecules (proteins, polymers), bacteria, and process monitoring. The successfully designed oligo(arylene ethynylene)-based sensors can be used as selective probes to detect particular analytes in the mixture and they can be used for selective process monitoring. However, their huge potential has not been explored, yet.

Well-defined conjugated arylene ethynylene can be accessed by iterative chemistry protocols that permit for full structure precision and sequence definition. The solubility issues occurring for oligo(arylene ethynylene)s can be overcome by the synthesis approach that uses soluble support. Nevertheless, the high synthesis scale and yields remain a challenge.

The sensing parameters (sensitivity, selectivity, specificity) are strongly connected with the oligomer structure. Even a small difference in structure, e.g., one unit length difference may result in loss of sensor selectivity and sensitivity. Although a variety of examples were described, it has been still difficult to rationally design the arylene ethynylene oligomers with high selectivity and affinity, though more systematic studies in the field are needed.

In the near future sensing and process monitoring can become an interesting and emerging application for sequence-defined polymers built from π-conjugated segments. As it was shown by many examples in this review sensing is one of the applications where monomer sequence, composition, and length matter. Systematic studies on the sequence–property relationship can open an avenue for more specific and selective sensors relevant to biological samples.

References

1. Biechele, P.; Busse, C.; Solle, D.; Scheper, T.; Reardon, K. Sensor systems for bioprocess monitoring. *Eng. Life Sci.* **2015**, *15*, 469–488. [CrossRef]
2. Vabret, N.; Bhardwaj, N.; Greenbaum, B.D. Sequence-Specific Sensing of Nucleic Acids. *Trends Immunol.* **2017**, *38*, 53–65. [CrossRef]
3. Lee, M.J.; Yaffe, M.B. Protein Regulation in Signal Transduction. *CSH Perspect. Biol.* **2016**, *8*, a005918. [CrossRef]
4. Scheer, P.V.D.; Laar, T.V.D.; Sprakel, J. Chain length-dependent luminescence in acceptor-doped conjugated polymers. *Sci. Rep.* **2019**, *9*, 11217. [CrossRef]
5. Lutz, J.-F.; Lehn, J.-M.; Meijer, E.W.; Matyjaszewski, K. From precision polymers to complex materials and systems. *Nat. Rev. Mater.* **2016**, *1*, 16024. [CrossRef]
6. Szweda, R.; Chendo, C.; Charles, L.; Baxter, P.N.W.; Lutz, J.-F. Synthesis of oligoarylacetylenes with defined conjugated sequences using tailor-made soluble polymer supports. *Chem. Commun.* **2017**, *53*, 8312–8315. [CrossRef]
7. Young, J.K.; Nelson, J.C.; Moore, J.S. Synthesis of Sequence Specific Phenylacetylene Oligomers on an Insoluble Solid Support. *J. Am. Chem. Soc.* **1994**, *116*, 10841–10842. [CrossRef]
8. Lavastre, O.; Ollivier, L.; Dixneuf, P.H.; Sibandhit, S. Sequential catalytic synthesis of rod-like conjugated poly-ynes. *Tetrahedron* **1996**, *52*, 5495–5504. [CrossRef]
9. Jones, L.; Schumm, J.S.; Tour, J.M. Rapid Solution and Solid Phase Syntheses of Oligo(1,4-phenylene ethynylene)s with Thioester Termini: Molecular Scale Wires with Alligator Clips. Derivation of Iterative Reaction Efficiencies on a Polymer Support. *J. Org. Chem.* **1997**, *62*, 1388–1410. [CrossRef]

10. Anderson, S. Phenylene Ethynylene Pentamers for Organic Electroluminescence. *Chem. Eur. J.* **2001**, *7*, 4706–4714. [CrossRef]

11. Elliott, E.L.; Ray, C.R.; Kraft, S.; Atkins, J.R.; Moore, J.S. Solid-Phase Synthesis of m-Phenylene Ethynylene Heterosequence Oligomers. *J. Org. Chem.* **2006**, *71*, 5282–5290. [CrossRef]

12. Schneider, R.V.; Waibel, K.A.; Arndt, A.P.; Lang, M.; Seim, R.; Busko, D.; Bräse, S.; Lemmer, U.; Meier, M.A.R. Sequence-definition in stiff conjugated oligomers. *Sci. Rep.* **2018**, *8*, 17483. [CrossRef]

13. Norris, B.N.; Zhang, S.; Campbell, C.M.; Auletta, J.T.; Calvo-Marzal, P.; Hutchison, G.R.; Meyer, T.Y. Sequence Matters: Modulating Electronic and Optical Properties of Conjugated Oligomers via Tailored Sequence. *Macromolecules* **2013**, *46*, 1384–1392. [CrossRef]

14. Zhang, S.; Bauer, N.E.; Kanal, I.Y.; You, W.; Hutchison, G.R.; Meyer, T.Y. Sequence Effects in Donor–Acceptor Oligomeric Semiconductors Comprising Benzothiadiazole and Phenylenevinylene Monomers. *Macromolecules* **2017**, *50*, 151–161. [CrossRef]

15. Zhang, S.; Hutchison, G.R.; Meyer, T.Y. Sequence Effects in Conjugated Donor–Acceptor Trimers and Polymers. *Macromol. Rapid Commun.* **2016**, *37*, 882–887. [CrossRef]

16. Nishide, Y.; Osuga, H.; Saito, M.; Aiba, T.; Inagaki, Y.; Doge, Y.; Tanaka, K. Synthesis and Properties of a Series of Well-Defined and Polydisperse Benzo[1,2-b:4,3-b′]dithiophene Oligomers. *J. Org. Chem.* **2007**, *72*, 9141–9151. [CrossRef]

17. Wang, S.; Liu, B.; Gaylord, B.S.; Bazan, G.C. Size-Specific Interactions Between Single- and Double-Stranded Oligonucleotides and Cationic Water-Soluble Oligofluorenes. *Adv. Funct. Mater.* **2003**, *13*, 463–467. [CrossRef]

18. Liu, B.; Gaylord, B.S.; Wang, S.; Bazan, G.C. Effect of Chromophore-Charge Distance on the Energy Transfer Properties of Water-Soluble Conjugated Oligomers. *J. Am. Chem. Soc.* **2003**, *125*, 6705–6714. [CrossRef]

19. Lawrence, J.; Goto, E.; Ren, J.M.; McDearmon, B.; Kim, D.S.; Ochiai, Y.; Clark, P.G.; Laitar, D.; Higashihara, T.; Hawker, C.J. A Versatile and Efficient Strategy to Discrete Conjugated Oligomers. *J. Am. Chem. Soc.* **2017**, *139*, 13735–13739. [CrossRef]

20. Johansson, L.B.G.; Simon, R.; Bergström, G.; Eriksson, M.; Prokop, S.; Mandenius, C.-F.; Heppner, F.L.; Åslund, A.K.O.; Nilsson, K.P.R. An azide functionalized oligothiophene ligand—A versatile tool for multimodal detection of disease associated protein aggregates. *Biosens. Bioelectron.* **2015**, *63*, 204–211. [CrossRef] [PubMed]

21. Sun, T.; Niu, Q.; Li, Y.; Li, T.; Hu, T.; Wang, E.; Liu, H. A novel oligothiophene-based colorimetric and fluorescent "turn on" sensor for highly selective and sensitive detection of cyanide in aqueous media and its practical applications in water and food samples. *Sens. Actuators B Chem.* **2018**, *258*, 64–71. [CrossRef]

22. Lan, L.; Li, T.; Wei, T.; Pang, H.; Sun, T.; Wang, E.; Liu, H.; Niu, Q. Oligothiophene-based colorimetric and ratiometric fluorescence dual-channel cyanide chemosensor: Sensing ability, TD-DFT calculations and its application as an efficient solid state sensor. *Spectrochim. Acta A* **2018**, *193*, 289–296. [CrossRef] [PubMed]

23. Miao, R.; Peng, J.; Fang, Y. Recent advances in fluorescent film sensing from the perspective of both molecular design and film engineering. *Mol. Syst. Des. Eng.* **2016**, *1*, 242–257. [CrossRef]

24. Freudenberg, J.; Hinkel, F.; Jänsch, D.; Bunz, U.H.F. Chemical Tongues and Noses Based upon Conjugated Polymers. *Top. Curr. Chem.* **2017**, *375*, 67. [CrossRef] [PubMed]

25. Geng, Y.; Peveler, W.J.; Rotello, V.M. Array-based "Chemical Nose" Sensing in Diagnostics and Drug Discovery. *Angew. Chem. Int. Ed.* **2019**, *58*, 5190–5200. [CrossRef] [PubMed]

26. Feng, F.; Liu, L.; Yang, Q.; Wang, S. Water-Soluble Conjugated Polymers for Fluorescent-Enzyme Assays. *Macromol. Rapid Commun.* **2010**, *31*, 1405–1421. [CrossRef]

27. Chen, Z.; Wang, Q.; Wu, X.; Li, Z.; Jiang, Y.-B. Optical chirality sensing using macrocycles, synthetic and supramolecular oligomers/polymers, and nanoparticle based sensors. *Chem. Soc. Rev.* **2015**, *44*, 4249–4263. [CrossRef]

28. Kubota, R.; Hamachi, I. Protein recognition using synthetic small-molecular binders toward optical protein sensing in vitro and in live cells. *Chem. Soc. Rev.* **2015**, *44*, 4454–4471. [CrossRef]

29. Ahner, J.; Pretzel, D.; Enke, M.; Geitner, R.; Zechel, S.; Popp, J.; Schubert, U.S.; Hager, M.D. Conjugated Oligomers as Fluorescence Marker for the Determination of the Self-Healing Efficiency in Mussel-Inspired Polymers. *Chem. Mater.* **2018**, *30*, 2791–2799. [CrossRef]

30. Wang, B.; Queenan, B.N.; Wang, S.; Nilsson, K.P.R.; Bazan, G.C. Precisely Defined Conjugated Oligoelectrolytes for Biosensing and Therapeutics. *Adv. Mater.* **2019**, *31*, 1806701. [CrossRef]

31. Li, Z.; Askim, J.R.; Suslick, K.S. The Optoelectronic Nose: Colorimetric and Fluorometric Sensor Arrays. *Chem. Rev.* **2019**, *119*, 231–292. [CrossRef] [PubMed]

32. Bunz, U.H.F. Poly(aryleneethynylene)s: Syntheses, Properties, Structures, and Applications. *Chem. Rev.* **2000**, *100*, 1605–1644. [CrossRef] [PubMed]

33. Wang, H.; Cui, H.; Liu, X.; Li, L.; Cao, Y.; Liu, T.; Fang, Y. Alternative Copolymerization of a Conjugated Segment and a Flexible Segment and Fabrication of a Fluorescent Sensing Film for HCl in the Vapor Phase. *Chem. Asian J.* **2013**, *8*, 101–107. [CrossRef] [PubMed]

34. Zyryanov, G.V.; Kopchuk, D.S.; Kovalev, I.S.; Nosova, E.V.; Rusinov, V.L.; Chupakhin, O.N. Chemosensors for detection of nitroaromatic compounds (explosives). *Russ. Chem. Rev.* **2014**, *83*, 783–819. [CrossRef]

35. Whitten, D.G.; Tang, Y.; Zhou, Z.; Yang, J.; Wang, Y.; Hill, E.H.; Pappas, H.C.; Donabedian, P.L.; Chi, E.Y. A Retrospective: 10 Years of Oligo(phenylene-ethynylene) Electrolytes: Demystifying Nanomaterials. *Langmuir* **2019**, *35*, 307–325. [CrossRef]

36. Lehnherr, D.; Chen, C.; Pedramrazi, Z.; DeBlase, C.R.; Alzola, J.M.; Keresztes, I.; Lobkovsky, E.B.; Crommie, M.F.; Dichtel, W.R. Sequence-defined oligo(ortho-arylene) foldamers derived from the benzannulation of ortho(arylene ethynylene)s. *Chem. Sci.* **2016**, *7*, 6357–6364. [CrossRef]

37. Löffler, S.; Antypas, H.; Choong, F.X.; Nilsson, K.P.R.; Richter-Dahlfors, A. Conjugated Oligo- and Polymers for Bacterial Sensing. *Front. Chem.* **2019**, *7*. [CrossRef]

38. Mulla, K.; Dongare, P.; Zhou, N.; Chen, G.; Thompson, D.W.; Zhao, Y. Highly sensitive detection of saccharides under physiological conditions with click synthesized boronic acid-oligomer fluorophores. *Org. Biomol. Chem.* **2011**, *9*, 1332–1336. [CrossRef]

39. Bunz, U.H.F.; Seehafer, K.; Bender, M.; Porz, M. Poly(aryleneethynylene)s (PAE) as paradigmatic sensor cores. *Chem. Soc. Rev.* **2015**, *44*, 4322–4336. [CrossRef]

40. Mako, T.L.; Racicot, J.M.; Levine, M. Supramolecular Luminescent Sensors. *Chem. Rev.* **2019**, *119*, 322–477. [CrossRef]

41. Lutz, J.-F.; Ouchi, M.; Liu, D.R.; Sawamoto, M. Sequence-Controlled Polymers. *Science* **2013**, *341*, 1238149. [CrossRef] [PubMed]

42. Solleder, S.C.; Schneider, R.V.; Wetzel, K.S.; Boukis, A.C.; Meier, M.A.R. Recent Progress in the Design of Monodisperse, Sequence-Defined Macromolecules. *Macromol. Rapid Commun.* **2017**, *38*, 1600711. [CrossRef] [PubMed]

43. Lutz, J.-F. Defining the Field of Sequence-Controlled Polymers. *Macromol. Rapid Commun.* **2017**, *38*, 1700582. [CrossRef] [PubMed]

44. De Neve, J.; Haven, J.J.; Maes, L.; Junkers, T. Sequence-definition from controlled polymerization: The next generation of materials. *Polym. Chem.* **2018**, *9*, 4692–4705. [CrossRef]

45. Feng, H.-T.; Yuan, Y.-X.; Xiong, J.-B.; Zheng, Y.-S.; Tang, B.Z. Macrocycles and cages based on tetraphenylethylene with aggregation-induced emission effect. *Chem. Soc. Rev.* **2018**, *47*, 7452–7476. [CrossRef] [PubMed]

46. Wong, C.-H.; Zimmerman, S.C. Orthogonality in organic, polymer, and supramolecular chemistry: From Merrifield to click chemistry. *Chem. Commun.* **2013**, *49*, 1679–1695. [CrossRef] [PubMed]

47. Cavallo, G.; Al Ouahabi, A.; Oswald, L.; Charles, L.; Lutz, J.-F. Orthogonal Synthesis of "Easy-to-Read" Information-Containing Polymers Using Phosphoramidite and Radical Coupling Steps. *J. Am. Chem. Soc.* **2016**, *138*, 9417–9420. [CrossRef]

48. Hill, S.A.; Gerke, C.; Hartmann, L. Recent Developments in Solid-Phase Strategies towards Synthetic, Sequence-Defined Macromolecules. *Chem. Asian J.* **2018**, *13*, 3611–3622. [CrossRef]

49. Trinh, T.T.; Laure, C.; Lutz, J.-F. Synthesis of Monodisperse Sequence-Defined Polymers Using Protecting-Group-Free Iterative Strategies. *Macromol. Chem. Phys.* **2015**, *216*, 1498–1506. [CrossRef]

50. Tour, J.M. Conjugated Macromolecules of Precise Length and Constitution. Organic Synthesis for the Construction of Nanoarchitectures. *Chem. Rev.* **1996**, *96*, 537–554. [CrossRef]

51. Zhang, L.; Colella, N.S.; Cherniawski, B.P.; Mannsfeld, S.C.B.; Briseno, A.L. Oligothiophene Semiconductors: Synthesis, Characterization, and Applications for Organic Devices. *ACS Appl. Mater.* **2014**, *6*, 5327–5343. [CrossRef] [PubMed]

52. Koch, F.P.V.; Smith, P.; Heeney, M. "Fibonacci's Route" to Regioregular Oligo(3-hexylthiophene)s. *J. Am. Chem. Soc.* **2013**, *135*, 13695–13698. [CrossRef] [PubMed]

53. Ten Hoeve, W.; Wynberg, H.; Havinga, E.E.; Meijer, E.W. Substituted 2,2′:5′,2″:5″,2‴:5‴,2⁗:5⁗,2″″′: 5″″′,2″″″:5″″″,2″″″′:5″″″′,2″″″″:5″″″″,2″″″″′:5″″″″′,2″″″″″-undecithiophenes, the longest characterized oligothiophenes. *J. Am. Chem. Soc.* **1991**, *113*, 5887–5889. [CrossRef]

54. Schumm, J.S.; Pearson, D.L.; Tour, J.M. Iterative Divergent/Convergent Approach to Linear Conjugated Oligomers by Successive Doubling of the Molecular Length: A Rapid Route to a 128Å-Long Potential Molecular Wire. *Angew. Chem. Int. Ed.* **1994**, *33*, 1360–1363. [CrossRef]

55. Huang, S.; Tour, J.M. Rapid bi-directional synthesis of oligo(1, 4-phenylene ethynylene)s. *Tetrahedron Lett.* **1999**, *40*, 3447–3450. [CrossRef]

56. Vonk, E.C.; Langeveld-Voss, B.M.W.; van Dongen, J.L.J.; Janssen, R.A.J.; Claessens, H.A.; Cramers, C.A. Separation and characterization of oligomers by reversed-phase high-performance liquid chromatography; a study on well-defined oligothiophenes. *J. Chromatogr. A* **2001**, *911*, 13–26. [CrossRef]

57. Advincula, R.C. Review of Conjugated Polymer Synthesis: Methods and Reactions. *J. Am. Chem. Soc.* **2011**, *133*, 5622. [CrossRef]

58. Kline, R.J.; McGehee, M.D.; Kadnikova, E.N.; Liu, J.; Fréchet, J.M.J. Controlling the Field-Effect Mobility of Regioregular Polythiophene by Changing the Molecular Weight. *Adv. Mater.* **2003**, *15*, 1519–1522. [CrossRef]

59. Pingel, P.; Zen, A.; Neher, D.; Lieberwirth, I.; Wegner, G.; Allard, S.; Scherf, U. Unexpectedly high field-effect mobility of a soluble, low molecular weight oligoquaterthiophene fraction with low polydispersity. *Appl. Phys. A* **2009**, *95*, 67–72. [CrossRef]

60. Lan, Y.-K.; Huang, C.-I. Charge Mobility and Transport Behavior in the Ordered and Disordered States of the Regioregular Poly(3-hexylthiophene). *J. Phys. Chem. B* **2009**, *113*, 14555–14564. [CrossRef]

61. Fanni, A.M.; Monge, F.A.; Lin, C.-Y.; Thapa, A.; Bhaskar, K.; Whitten, D.G.; Chi, E.Y. High Selectivity and Sensitivity of Oligomeric p-Phenylene Ethynylenes for Detecting Fibrillar and Prefibrillar Amyloid Protein Aggregates. *ACS Chem. Neurosci.* **2019**, *10*, 1813–1825. [CrossRef] [PubMed]

62. Abe, H.; Machiguchi, H.; Matsumoto, S.; Inouye, M. Saccharide Recognition-Induced Transformation of Pyridine−Pyridone Alternate Oligomers from Self-Dimer to Helical Complex. *J. Org. Chem.* **2008**, *73*, 4650–4661. [CrossRef]

63. Adachi, N.; Yoshinari, M.; Suzuki, E.; Okada, M. Oligo(p-phenylene ethynylene) with Cyanoacrylate Terminal Groups and Graphene Composite as Fluorescent Chemical Sensor for Cysteine. *J. Fluoresc.* **2017**, *27*, 1449–1456. [CrossRef]

64. De los Santos, Z.A.; Yusin, G.; Wolf, C. Enantioselective sensing of carboxylic acids with a bis(urea)oligo(phenylene)ethynylene foldamer. *Tetrahedron* **2019**, *75*, 1504–1509. [CrossRef]

65. Suk, J.-M.; Kim, D.A.; Jeong, K.-S. Helicity Control of an Indolocarbazole Foldamer by Chiral Organic Anions. *Org. Lett.* **2012**, *14*, 5018–5021. [CrossRef] [PubMed]

66. Reiné, P.; Justicia, J.; Morcillo, S.P.; Abbate, S.; Vaz, B.; Ribagorda, M.; Orte, Á.; Álvarez de Cienfuegos, L.; Longhi, G.; Campaña, A.G.; et al. Pyrene-Containing ortho-Oligo(phenylene)ethynylene Foldamer as a Ratiometric Probe Based on Circularly Polarized Luminescence. *J. Org. Chem.* **2018**, *83*, 4455–4463. [CrossRef] [PubMed]

67. Yang, J.-S.; Yan, J.-L.; Hwang, C.-Y.; Chiou, S.-Y.; Liau, K.-L.; Gavin Tsai, H.-H.; Lee, G.-H.; Peng, S.-M. Probing the Intrachain and Interchain Effects on the Fluorescence Behavior of Pentiptycene-Derived Oligo(p-phenyleneethynylene)s. *J. Am. Chem. Soc.* **2006**, *128*, 14109–14119. [CrossRef]

68. Feng, F.; Yang, J.; Xie, D.; McCarley, T.D.; Schanze, K.S. Remarkable Photophysics and Amplified Quenching of Conjugated Polyelectrolyte Oligomers. *J. Phys. Chem. Lett.* **2013**, *4*, 1410–1414. [CrossRef]

69. Phillips, R.L.; Miranda, O.R.; You, C.-C.; Rotello, V.M.; Bunz, U.H.F. Rapid and Efficient Identification of Bacteria Using Gold-Nanoparticle–Poly(para-phenyleneethynylene) Constructs. *Angew. Chem. Int. Ed.* **2008**, *47*, 2590–2594. [CrossRef]

70. George, W.N.; Giles, M.; McCulloch, I.; Steinke, J.H.G.; deMello, J.C. Efficient Quenching of a Guanidinium-Containing Fluorescence Sensor. *ChemPhysChem* **2011**, *12*, 765–768. [CrossRef]

71. Hill, E.H.; Goswami, S.; Evans, D.G.; Schanze, K.S.; Whitten, D.G. Photochemistry of a Model Cationic p-Phenylene Ethynylene in Water. *J. Phys. Chem. Lett.* **2012**, *3*, 1363–1368. [CrossRef] [PubMed]

72. Hill, E.H.; Evans, D.G.; Whitten, D.G. The influence of structured interfacial water on the photoluminescence of carboxyester-terminated oligo-p-phenylene ethynylenes. *J. Phys. Org. Chem.* **2014**, *27*, 252–257. [CrossRef]

73. Donabedian, P.L.; Pham, T.K.; Whitten, D.G.; Chi, E.Y. Oligo(p-phenylene ethynylene) Electrolytes: A Novel Molecular Scaffold for Optical Tracking of Amyloids. *ACS Chem. Neurosci.* **2015**, *6*, 1526–1535. [CrossRef] [PubMed]

74. Hill, E.H.; Zhang, Y.; Evans, D.G.; Whitten, D.G. Enzyme-Specific Sensors via Aggregation of Charged p-Phenylene Ethynylenes. *ACS Appl. Mater.* **2015**, *7*, 5550–5560. [CrossRef] [PubMed]

75. Hill, E.H.; Sanchez, D.; Evans, D.G.; Whitten, D.G. Structural Basis for Aggregation Mode of oligo-p-Phenylene Ethynylenes with Ionic Surfactants. *Langmuir* **2013**, *29*, 15732–15737. [CrossRef]

76. Donabedian, P.L.; Creyer, M.N.; Monge, F.A.; Schanze, K.S.; Chi, E.Y.; Whitten, D.G. Detergent-induced self-assembly and controllable photosensitizer activity of diester phenylene ethynylenes. *Proc. Natl. Acad. Sci. USA* **2017**, *114*, 7278–7282. [CrossRef] [PubMed]

77. Tang, Y.; Zhou, Z.; Ogawa, K.; Lopez, G.P.; Schanze, K.S.; Whitten, D.G. Photophysics and self-assembly of symmetrical and unsymmetrical cationic oligophenylene ethynylenes. *J. Photochem. Photobiol. A* **2009**, *207*, 4–6. [CrossRef]

78. Tang, Y.; Zhou, Z.; Ogawa, K.; Lopez, G.P.; Schanze, K.S.; Whitten, D.G. Synthesis, Self-Assembly, and Photophysical Behavior of Oligo Phenylene Ethynylenes: From Molecular to Supramolecular Properties. *Langmuir* **2009**, *25*, 21–25. [CrossRef]

79. Tang, Y.; Corbitt, T.S.; Parthasarathy, A.; Zhou, Z.; Schanze, K.S.; Whitten, D.G. Light-Induced Antibacterial Activity of Symmetrical and Asymmetrical Oligophenylene Ethynylenes. *Langmuir* **2011**, *27*, 4956–4962. [CrossRef]

80. Tong, W.-L.; Lai, L.-M.; Chan, M.C.W. Platinum(ii) Schiff base as versatile phosphorescent core component in conjugated oligo(phenylene–ethynylene)s. *Dalton Trans.* **2008**, *1*, 1412–1414. [CrossRef]

81. Arias, E.; Méndez, M.T.; Arias, E.; Moggio, I.; Ledezma, A.; Romero, J.; Margheri, G.; Giorgetti, E. Supramolecular Recognition of Escherichia coli Bacteria by Fluorescent Oligo(Phenyleneethynylene)s with Mannopyranoside Termini Groups. *Sensors* **2017**, *17*, 1025. [CrossRef] [PubMed]

82. Concepción García, M.; Turlakov, G.; Moggio, I.; Arias, E.; Valenzuela, J.H.; Hernández, M.; Rodríguez, G.; Ziolo, R.F. Synthesis and photophysical properties of conjugated (dodecyl)benzoateethynylene macromolecules: Staining of Bacillus subtilis and Escherichia coli rhizobacteria. *New J. Chem.* **2019**, *43*, 3332–3340. [CrossRef]

83. Barata, P.D.; Prata, J.V. New entities for sensory chemistry based on calix[4]arene-carbazole conjugates: From synthesis to applications. *Supramol. Chem.* **2013**, *25*, 782–797. [CrossRef]

84. Caron, T.; Guillemot, M.; Montméat, P.; Veignal, F.; Perraut, F.; Prené, P.; Serein-Spirau, F. Ultra trace detection of explosives in air: Development of a portable fluorescent detector. *Talanta* **2010**, *81*, 543–548. [CrossRef]

85. Cui, H.; He, G.; Wang, H.; Sun, X.; Liu, T.; Ding, L.; Fang, Y. Fabrication of a Novel Cholic Acid Modified OPE-Based Fluorescent Film and Its Sensing Performances to Inorganic Acids in Acetone. *ACS Appl. Mater.* **2012**, *4*, 6935–6941. [CrossRef]

86. Imsick, B.G.; Acharya, J.R.; Nesterov, E.E. Surface-Immobilized Monolayers of Conjugated Oligomers as a Platform for Fluorescent Sensors Design: The Effect of Exciton Delocalization on Chemosensing Performance. *Adv. Mater.* **2013**, *25*, 120–124. [CrossRef]

87. Wang, H.; He, G.; Chen, X.; Liu, T.; Ding, L.; Fang, Y. Cholesterol modified OPE functionalized film: Fabrication, fluorescence behavior and sensing performance. *J. Mater. Chem.* **2012**, *22*, 7529–7536. [CrossRef]

88. Xin, J.-G.; Yang, C.-L.; Wang, M.-S.; Ma, X.-G. OPE molecular junction as a hydrogen gas sensor. *Curr. Appl. Phys.* **2018**, *18*, 273–279. [CrossRef]

89. Li, H.B.; Tebikachew, B.E.; Wiberg, C.; Moth-Poulsen, K.; Hihath, J. A Memristive Element based on Electrically Controlled Single-Molecule Reaction. *Angew. Chem. Int. Ed.* **2020**. [CrossRef]

90. Deng, J.; Liu, M.; Lin, F.; Zhang, Y.; Liu, Y.; Yao, S. Self-assembled oligo(phenylene ethynylene)s/graphene nanocomposite with improved electrochemical performances for dopamine determination. *Anal. Chim. Acta* **2013**, *767*, 59–65. [CrossRef]

91. Samanta, D.; Singh, A.; Verma, P.; Bhattacharyya, S.; Roy, S.; Maji, T.K. Photoswitchable J-Aggregated Processable Organogel by Integrating a Photochromic Acceptor. *J. Org. Chem.* **2019**, *84*, 10946–10952. [CrossRef] [PubMed]

92. Pappas, H.C.; Donabedian, P.L.; Schanze, K.S.; Whitten, D.G. Intended and Unintended Consequences and Applications of Unnatural Interfaces: Oligo p-Phenylene Ethynylene Electrolytes, Biological Cells and Biomacromolecules. *J. Braz. Chem. Soc.* **2016**, *27*, 256–266. [CrossRef]

93. Zhao, X.; Liu, Y.; Schanze, K.S. A conjugated polyelectrolyte-based fluorescence sensor for pyrophosphate. *Chem. Commun.* **2007**, *1*, 2914–2916. [CrossRef] [PubMed]

94. Ávila-Rovelo, N.R.; Ruiz-Carretero, A. Recent Progress in Hydrogen-Bonded π-Conjugated Systems Displaying J-Type Aggregates. *Org. Mater.* **2020**, *2*, 47–63. [CrossRef]

95. Dascier, D.; Ji, E.; Parthasarathy, A.; Schanze, K.S.; Whitten, D.G. Efficacy of End-Only-Functionalized Oligo(arylene-ethynylene)s in Killing Bacterial Biofilms. *Langmuir* **2012**, *28*, 11286–11290. [CrossRef] [PubMed]

96. Robinson, H.D.; Montazami, R.; Daengngam, C.; Zuo, Z.; Dong, W.; Metzman, J.; Heflin, R. Optoelectronic Materials and Devices Incorporating Polyelectrolyte Multilayers. In *Multilayer Thin Films*; Decher, G., Schlenoff, J.B., Eds.; Wiley-VCH Verlag GmbH & Co. KGaA: Weinheim, Germany, 2012; pp. 511–537.

97. Shrivastava, S.; Jadon, N.; Jain, R. Next-generation polymer nanocomposite-based electrochemical sensors and biosensors: A review. *TrAC Trends Anal. Chem.* **2016**, *82*, 55–67. [CrossRef]